

$B \rightarrow a_1(1260)a_1(1260)$ and $b_1(1235)b_1(1235)$ decays in the perturbative QCD approach

Xin Liu^{1a} and Zhen-Jun Xiao^{2b}

¹ *School of Physics and Electronic Engineering, Jiangsu Normal University, Xuzhou, Jiangsu 221116, People's Republic of China*

² *Department of Physics and Institute of Theoretical Physics, Nanjing Normal University, Nanjing, Jiangsu 210046, People's Republic of China*

(Dated: May 26, 2018)

Abstract

In this work, we study six tree-dominated $B \rightarrow a_1(1260)a_1(1260)$ and $b_1(1235)b_1(1235)$ decays in the perturbative QCD(pQCD) approach, where $a_1(b_1)$ is a $^3P_1(^1P_1)$ axial-vector meson. Based on the perturbative calculations and phenomenological analysis, we find that: (a) the CP-averaged branching ratio of $B^0 \rightarrow a_1^+ a_1^-$ decay in the pQCD approach is 54.7×10^{-6} , which agrees well with the current data and the predictions given in the QCD factorization approach within errors; (b) the numerical results for the decay rates of other five channels are found to be in the order of $10^{-6} \sim 10^{-5}$, which could be accessed at B factories and Large Hadron Collider(LHC) experiments; (c) other physical observables such as polarization fractions and direct CP-violating asymmetries are also investigated with the pQCD approach in the present work and the predictions can be confronted with the relevant experiments in the near future; (d) the different phenomenologies shown between $B \rightarrow a_1 a_1$ and $B \rightarrow b_1 b_1$ decays are expected to be tested by the ongoing LHC and forthcoming Super-B experiments, which could shed light on the typical QCD dynamics involved in these decay modes, as well as in 3P_1 meson a_1 and 1P_1 meson b_1 .

PACS numbers: 13.25.Hw, 12.38.Bx, 14.40.Nd

^a Electronic address: liuxin.physics@gmail.com

^b Electronic address: xiaozhenjun@njnu.edu.cn

I. INTRODUCTION

Charmless B meson decays to final states involving two axial-vector mesons (AA) have attracted attentions in theory and experiments in the last few years [1–7]. It is expected that through the study of $B \rightarrow AA$ decays, the issues related with the internal structure, such as the angles between the mixtures of 3P_1 and/or 1P_1 states [8, 9], of the light axial-vector mesons can receive new understanding. On one hand, $B \rightarrow AA$ will open another window to study their physical properties; The CP asymmetries of these decays, on the other hand, shall provide another way to measure the Cabibbo-Kobayashi-Maskawa (CKM) angles β and α . Furthermore, analogous to $B \rightarrow VV$ decays, being constructed of three polarization states, the charmless B decays to AA mesons are expected to have rich physics and provide much more information on the underlying helicity structure of the decay mechanism through polarization studies [3].

Very recently, the measurement on branching ratio(BR) and fraction of longitudinal polarization(f_L) for $B^0 \rightarrow a_1(1260)^+ a_1(1260)^-$ [5, 10] decay has been reported by BaBar Collaboration,

$$\text{BR}(B^0 \rightarrow a_1(1260)^+ a_1(1260)^-)_{\text{Exp.}} = 47.3 \pm 12.2 \times 10^{-6} ; \quad (1)$$

$$f_L(B^0 \rightarrow a_1(1260)^+ a_1(1260)^-)_{\text{Exp.}} = 0.31 \pm 0.24 . \quad (2)$$

with large uncertainties. However, this measurement will be improved rapidly with the running of Large Hadron Collider(LHC) experiments, in which the events of B mesons are expected to be produced more than those collected in the B factories by about 3 orders per year.

On the theory side, $B \rightarrow a_1 a_1^1$ decays have been studied in the literature [2–4], but the predictions on BRs of the considered channels are significantly different from each other by employing the approach with naive factorization [11] and QCD factorization(QCDF) [12], respectively. For $B^0 \rightarrow a_1^+ a_1^-$ mode, for example, the branching ratio predicted in naive factorization is 6.4×10^{-6} [2], while that presented in QCDF is 37.4×10^{-6} [3]. One can easily see that the former result is too small to be confronted with the preliminary data and the latter one going beyond the naive factorization is large enough to be compatible with the measurements. As the counterparts of $B \rightarrow a_1 a_1$ decays, $B \rightarrow b_1 b_1$ modes have also been investigated within the framework of QCDF [3] and the BRs are found to be in the order of $10^{-6} \sim 10^{-5}$ within large uncertainties. More important, an interesting pattern of the BRs for $B \rightarrow b_1 b_1$ decays is exhibited through the calculations based on QCDF in Ref. [3], i.e., $\text{BR}(B^0 \rightarrow b_1^0 b_1^0) > \text{BR}(B^+ \rightarrow b_1^+ b_1^0) > \text{BR}(B^0 \rightarrow b_1^+ b_1^-)$, which is significantly contrary to that for $B \rightarrow a_1 a_1$ channels, i.e., $\text{BR}(B^0 \rightarrow a_1^0 a_1^0) < \text{BR}(B^+ \rightarrow a_1^+ a_1^0) < \text{BR}(B^0 \rightarrow a_1^+ a_1^-)$. Here, we want to mention that, as stated in Ref. [3], the troublesome endpoint singularities from hard spectator scattering and annihilation decay amplitudes always exist in the framework of QCDF and have to be determined through the input parameters fitted from the relevant precision measurements.

Inspired by the above interesting facts from both theoretical and experimental aspects, we here study $B \rightarrow a_1 a_1$ and $b_1 b_1$ decays in the present work by employing the low energy effective Hamiltonian [13] and the perturbative QCD(pQCD) approach [14, 15].

¹ Hereafter, for the sake of simplicity, we will adopt the forms a_1 and b_1 (to be shown below) to denote the meson $a_1(1260)$ and $b_1(1235)$ in the content, respectively, unless otherwise stated.

It is worth of stressing that the nonfactorizable spectator and annihilation diagrams are calculable perturbatively in the pQCD approach. Furthermore, the new measurements on the pure annihilation $B_s \rightarrow \pi^+ \pi^-$ decay reported by CDF [16] and LHCb [17] collaborations last year confirmed the previous pQCD predictions [18–20], while the measured large decay rate of $B^0 \rightarrow K^+ K^-$ also naturally explained by the renewed pQCD predictions [20].

Although a_1 and b_1 mesons embrace the same components at the quark level, because of different couplings of orbital and spin angular momenta, as explored in the QCD sum rule method [8], the hadron dynamics of b_1 is very different from that of its partner, a_1 . In our numerical evaluations, the different phenomenologies do appear between these considered $B \rightarrow a_1 a_1$ and $B \rightarrow b_1 b_1$ decays. Therefore, one could expect reasonably that more new information on the contents such as polarizations, CP asymmetries, CKM unitary angles, even the knowledge of color-suppressed processes in B meson decays [21–24] may be deduced through the detailed studies on $B \rightarrow a_1 a_1$ and $b_1 b_1$ decays. Moreover, the hadron dynamics could be implicated by these perturbative calculations with the help of precision measurements.

The paper is organized as follows. In Sec. II, we present the theoretical framework on the low energy effective Hamiltonian, formalism of pQCD approach and mesons' wave functions. Then we perform the perturbative calculations for $B \rightarrow a_1 a_1$ and $b_1 b_1$ decays in Sec. III. The analytic expressions of the decay amplitudes for the considered modes are also grouped in this section. The numerical results and phenomenological analysis are given in Sec. IV. The main conclusions and a short summary are presented in the last section.

II. THEORETICAL FRAMEWORK

For the considered $B \rightarrow a_1 a_1$ and $b_1 b_1$ decays with $\bar{b} \rightarrow \bar{d}$ transition, the related weak effective Hamiltonian H_{eff} [13] can be written as

$$H_{\text{eff}} = \frac{G_F}{\sqrt{2}} \left\{ V_{ub}^* V_{ud} [C_1(\mu) O_1^u(\mu) + C_2(\mu) O_2^u(\mu)] - V_{tb}^* V_{td} \sum_{i=3}^{10} C_i(\mu) O_i(\mu) \right\}, \quad (3)$$

with the Fermi constant $G_F = 1.16639 \times 10^{-5} \text{GeV}^{-2}$, CKM matrix elements V , and Wilson coefficients $C_i(\mu)$ at the renormalization scale μ . The local four-quark operators $O_i (i = 1, \dots, 10)$ are

$$\begin{aligned} O_1^u &= (\bar{d}_\alpha u_\beta)_{V-A} (\bar{u}_\beta b_\alpha)_{V-A}, & O_2^u &= (\bar{d}_\alpha u_\alpha)_{V-A} (\bar{u}_\beta b_\beta)_{V-A}; \\ O_3 &= (\bar{d}_\alpha b_\alpha)_{V-A} \sum_{q'} (\bar{q}'_\beta q'_\beta)_{V-A}, & O_4 &= (\bar{d}_\alpha b_\beta)_{V-A} \sum_{q'} (\bar{q}'_\beta q'_\alpha)_{V-A}, \\ O_5 &= (\bar{d}_\alpha b_\alpha)_{V-A} \sum_{q'} (\bar{q}'_\beta q'_\beta)_{V+A}, & O_6 &= (\bar{d}_\alpha b_\beta)_{V-A} \sum_{q'} (\bar{q}'_\beta q'_\alpha)_{V+A}; \\ O_7 &= \frac{3}{2} (\bar{d}_\alpha b_\alpha)_{V-A} \sum_{q'} e_{q'} (\bar{q}'_\beta q'_\beta)_{V+A}, & O_8 &= \frac{3}{2} (\bar{d}_\alpha b_\beta)_{V-A} \sum_{q'} e_{q'} (\bar{q}'_\beta q'_\alpha)_{V+A}, \\ O_9 &= \frac{3}{2} (\bar{d}_\alpha b_\alpha)_{V-A} \sum_{q'} e_{q'} (\bar{q}'_\beta q'_\beta)_{V-A}, & O_{10} &= \frac{3}{2} (\bar{d}_\alpha b_\beta)_{V-A} \sum_{q'} e_{q'} (\bar{q}'_\beta q'_\alpha)_{V-A}. \end{aligned} \quad (4)$$

with the color indices α, β and the notations $(\bar{q}'q')_{V\pm A} = \bar{q}'\gamma_\mu(1 \pm \gamma_5)q'$. The index q' in the summation of the above operators runs through u, d, s, c , and b . Since we work in the leading order $[\mathcal{O}(\alpha_s)]$ of the pQCD approach, it is consistent to use the leading order Wilson coefficients. For the renormalization group evolution of the Wilson coefficients from higher scale to lower scale, we use the formulas as given in Ref. [14] directly.

The pQCD approach, one of the method based on QCD dynamics in the market, has been employed to treat two-body nonleptonic $B_{(s)}$ decays extensively. As a unique feature different from other two factorization approaches, i.e., QCDF and SCET (soft-collinear effective theory) [25], the pQCD approach is based on the framework of k_T factorization theorem with taking the tranverse momentum k_T , generally considered as a small and negligible scale, of the valence quarks in the hadrons into account, which results in the Sudakov factor smearing the endpoint singularities in the decay amplitude and makes the nonfactorizable spectator and annihilation diagrams perturbatively calculable, aside from the emission one.

Because of the rather heavy b quark, for convenience, we will work in the rest frame of B meson. Throughout this paper, we will use light-cone coordinate (P^+, P^-, \mathbf{P}_T) to describe the meson's momenta with the definitions

$$P^\pm = \frac{p_0 \pm p_3}{\sqrt{2}} \quad \text{and} \quad \mathbf{P}_T = (p_1, p_2); \quad (5)$$

Then for $B^0 \rightarrow a_1^+ a_1^-$ decay, for example, the involved three meson momenta in the light-cone coordinates can be written as

$$P_1 = \frac{m_B}{\sqrt{2}}(1, 1, \mathbf{0}_T), \quad P_2 = \frac{m_B}{\sqrt{2}}(1 - r_3^2, r_2^2, \mathbf{0}_T), \quad P_3 = \frac{m_B}{\sqrt{2}}(r_3^2, 1 - r_2^2, \mathbf{0}_T), \quad (6)$$

respectively, where the a_1^+ (a_1^-) meson moves in the plus (minus) z direction carrying the momentum P_2 (P_3) and $r_2 = r_3 = m_{a_1}/m_B$. The longitudinal and transverse polarization vectors of axial-vector meson are denoted by ϵ^L and ϵ^T , respectively, satisfying $P \cdot \epsilon = 0$ in each polarization. The longitudinal polarization vectors, ϵ_2^L and ϵ_3^L , can be chosen as

$$\epsilon_2^L = \frac{m_B}{\sqrt{2}m_{a_1}}(1 - r_3^2, -r_2^2, \mathbf{0}_T) \quad \text{and} \quad \epsilon_3^L = \frac{m_B}{\sqrt{2}m_{a_1}}(-r_3^2, 1 - r_2^2, \mathbf{0}_T). \quad (7)$$

And the transverse ones are parameterized as $\epsilon_2^T = (0, 0, \mathbf{1}_T)$ and $\epsilon_3^T = (0, 0, \mathbf{1}_T)$.

Putting the (light) quark momenta in B , a_1^+ and a_1^- mesons as k_1 , k_2 , and k_3 , respectively, we define

$$k_1 = (x_1 P_1^+, 0, \mathbf{k}_{1T}), \quad k_2 = (x_2 P_2^+, 0, \mathbf{k}_{2T}), \quad k_3 = (0, x_3 P_3^-, \mathbf{k}_{3T}). \quad (8)$$

Then, for $B^0 \rightarrow a_1^+ a_1^-$ decay, the integration over k_1^- , k_2^- , and k_3^+ will conceptually lead to the decay amplitude in the pQCD approach,

$$\mathcal{A}(B \rightarrow a_1^+ a_1^-) \sim \int dx_1 dx_2 dx_3 b_1 db_1 b_2 db_2 b_3 db_3 \cdot \text{Tr} \left[C(t) \Phi_B(x_1, b_1) \Phi_{a_1^+}(x_2, b_2) \Phi_{a_1^-}(x_3, b_3) H(x_i, b_i, t) S_t(x_i) e^{-S(t)} \right]. \quad (9)$$

where b_i is the conjugate space coordinate of k_{iT} , and t is the largest energy scale in function $H(x_i, b_i, t)$. The large logarithms $\ln(m_W/t)$ are included in the Wilson coefficients

$C(t)$. The large double logarithms ($\ln^2 x_i$) given rise from loop corrections to the weak decay vertex are summed by the threshold resummation [26], and they lead to $S_t(x_i)$ which can decrease faster than any power of x as $x \rightarrow 0$, then remove the endpoint singularities. The last term, $e^{-S(t)}$, is the Sudakov factor which suppresses the soft dynamics effectively [27]. Thus it makes the perturbative calculation of the hard part H applicable at intermediate scale, i.e., m_B scale. We will calculate analytically the function $H(x_i, b_i, t)$ for the considered decays at leading order in α_s expansion and give the convoluted amplitudes in next section.

The pQCD predictions depend on the inputs for the nonperturbative parameters such as the decay constants and distribution amplitudes. For heavy B meson, in principle, both Lorentz structures of the wave function should be considered in the calculations. However, the contribution induced by the second Lorentz structure is numerically small and approximately negligible [28], we therefore employ the following set of heavy B meson wave function [14],

$$\Phi_B(x, b) = \frac{i}{\sqrt{6}} \left[(\not{P} + m_B) \gamma_5 \phi_B(x, b) \right]_{\alpha\beta}, \quad (10)$$

where the distribution amplitude $\phi_B(x, b)$ has been modeled as [14],

$$\phi_B(x, b) = N_B x^2 (1-x)^2 \exp \left[-\frac{1}{2} \left(\frac{x m_B}{\omega_B} \right)^2 - \frac{\omega_B^2 b^2}{2} \right], \quad (11)$$

In recent years, the shape parameter ω_B in Eq. (11) has been fixed at 0.40 GeV in the pQCD approach by using the rich experimental data on the B mesons with $f_B = 0.19$ GeV. The normalization factor N_B is related to the decay constant f_B through

$$\int_0^1 dx \phi_B(x, b=0) = \frac{f_B}{2\sqrt{6}}. \quad (12)$$

Correspondingly, the normalization constant N_B is 91.745 for $\omega_B = 0.40$. To analyze the uncertainties of theoretical predictions induced by the inputs, we will vary the shape parameter ω_B by 10%.

For the wave functions of axial-vector a_1 and b_1 mesons, one longitudinal(L) and two transverse(T) polarizations are involved, and can be written as [29],

$$\Phi_A^L(x) = \frac{1}{\sqrt{6}} \gamma_5 \left\{ m_A \not{\epsilon}_A^{*L} \phi_A(x) + \not{\epsilon}_A^{*L} \not{P} \phi_A^t(x) + m_A \phi_A^s(x) \right\}_{\alpha\beta}, \quad (13)$$

$$\Phi_A^T(x) = \frac{1}{\sqrt{6}} \gamma_5 \left\{ m_A \not{\epsilon}_A^{*T} \phi_A^v(x) + \not{\epsilon}_A^{*T} \not{P} \phi_A^T(x) + m_A i \epsilon_{\mu\nu\rho\sigma} \gamma_5 \gamma^\mu \epsilon_T^{*\nu} n^\rho v^\sigma \phi_A^a(x) \right\}_{\alpha\beta}, \quad (14)$$

where x denotes the momentum fraction carried by quark in the meson, and $n = (1, 0, \mathbf{0}_T)$ and $v = (0, 1, \mathbf{0}_T)$ are dimensionless light-like unit vectors. We here adopt the convention $\epsilon^{0123} = 1$ for the Levi-Civita tensor $\epsilon^{\mu\nu\alpha\beta}$.

The twist-2 distribution amplitudes for the longitudinally and trasversely polarized axial-vector 3P_1 and 1P_1 mesons can be parameterized as [8, 29]:

$$\phi_A(x) = \frac{3f_A}{\sqrt{2N_c}} x(1-x) \left[a_{0A}^{\parallel} + 3a_{1A}^{\parallel} (2x-1) + a_{2A}^{\parallel} \frac{3}{2} (5(2x-1)^2 - 1) \right], \quad (15)$$

$$\phi_A^T(x) = \frac{3f_A}{\sqrt{2N_c}} x(1-x) \left[a_{0A}^{\perp} + 3a_{1A}^{\perp} (2x-1) + a_{2A}^{\perp} \frac{3}{2} (5(2x-1)^2 - 1) \right], \quad (16)$$

where f_A is the decay constant. Here, the definition of these distribution amplitudes $\phi_A(x)$ and $\phi_A^T(x)$ satisfy the following relations:

$$\begin{aligned} \int_0^1 \phi_{3P_1}(x) &= \frac{f_{3P_1}}{2\sqrt{2N_c}}, & \int_0^1 \phi_{3P_1}^T(x) &= a_{0^3P_1}^\perp \frac{f_{3P_1}}{2\sqrt{2N_c}}; \\ \int_0^1 \phi_{1P_1}(x) &= a_{0^1P_1}^\parallel \frac{f_{1P_1}}{2\sqrt{2N_c}}, & \int_0^1 \phi_{1P_1}^T(x) &= \frac{f_{1P_1}}{2\sqrt{2N_c}}. \end{aligned} \quad (17)$$

where $a_{0^3P_1}^\parallel = 1$ and $a_{0^1P_1}^\perp = 1$ have been used.

As for twist-3 distribution amplitudes for axial-vector meson, we use the following forms [29]:

$$\phi_A^t(x) = \frac{3f_A}{2\sqrt{2N_c}} \left\{ a_{0A}^\perp (2x-1)^2 + \frac{1}{2} a_{1A}^\perp (2x-1)(3(2x-1)^2 - 1) \right\}, \quad (18)$$

$$\phi_A^s(x) = \frac{3f_A}{2\sqrt{2N_c}} \frac{d}{dx} \left\{ x(1-x)(a_{0A}^\perp + a_{1A}^\perp(2x-1)) \right\}; \quad (19)$$

$$\phi_A^v(x) = \frac{3f_A}{4\sqrt{2N_c}} \left\{ \frac{1}{2} a_{0A}^\parallel (1 + (2x-1)^2) + a_{1A}^\parallel (2x-1)^3 \right\}, \quad (20)$$

$$\phi_A^a(x) = \frac{3f_A}{4\sqrt{2N_c}} \frac{d}{dx} \left\{ x(1-x)(a_{0A}^\parallel + a_{1A}^\parallel(2x-1)) \right\}. \quad (21)$$

The Gegenbauer moments $a_{i,A}^{||(\perp)}$ have been studied extensively in the literatures (see Ref. [8] and references therein), here we adopt the following values:

$$\begin{aligned} f_{a_1} &= 0.238 \pm 0.010 \text{ GeV}, & a_{2,a_1}^\parallel &= -0.02 \pm 0.02, & a_{1,a_1}^\perp &= -1.04 \pm 0.34; \\ f_{b_1} &= 0.180 \pm 0.008 \text{ GeV}, & a_{1,b_1}^\parallel &= -1.95 \pm 0.35, & a_{2,b_1}^\perp &= 0.03 \pm 0.19. \end{aligned} \quad (22)$$

Note that we have included the intrinsic b dependence for the heavy meson wave function ϕ_B but not for the light axial-vector meson wave function ϕ_A . It has been shown that the intrinsic b dependence of the light meson wave functions is not important and negligible [30, 31]. It is reasonable to preliminarily assume that the intrinsic b dependence of the a_1 and b_1 wave functions, which are still unknown, is not essential either.

III. PERTURBATIVE CALCULATIONS IN PQCD APPROACH

There are three kinds of polarizations of a axial-vector meson, namely, longitudinal (L), normal (N), and transverse (T). Analogous to the $B \rightarrow \rho\rho$ decays [32–34], the amplitudes for the $B \rightarrow a_1 a_1$ decays are also characterized by the polarization states of these axial-vector mesons. In terms of helicities, the decay amplitudes $\mathcal{M}^{(\sigma)}$ for $B \rightarrow a_1(P_2, \epsilon_2^*) a_1(P_3, \epsilon_3^*)$ decays can be generally described by

$$\begin{aligned} \mathcal{M}^{(\sigma)} &= \epsilon_{2\mu}^*(\sigma) \epsilon_{3\nu}^*(\sigma) \left[a g^{\mu\nu} + \frac{b}{m_{a_1} m_{a_1}} P_1^\mu P_1^\nu + i \frac{c}{m_{a_1} m_{a_1}} \epsilon^{\mu\nu\alpha\beta} P_{2\alpha} P_{3\beta} \right], \\ &\equiv m_B^2 \mathcal{M}_L + m_B^2 \mathcal{M}_N \epsilon_2^*(\sigma = T) \cdot \epsilon_3^*(\sigma = T) \\ &\quad + i \mathcal{M}_T \epsilon^{\alpha\beta\gamma\rho} \epsilon_{2\alpha}^*(\sigma) \epsilon_{3\beta}^*(\sigma) P_{2\gamma} P_{3\rho}, \end{aligned} \quad (23)$$

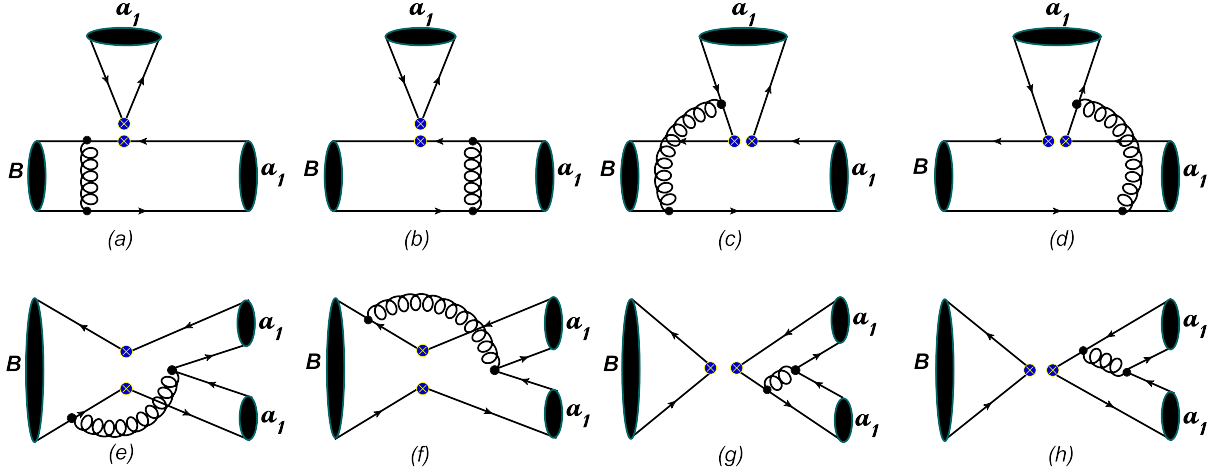


FIG. 1. (Color online) Typical Feynman diagrams for $B \rightarrow a_1 a_1$ decays at the lowest order in the pQCD approach. By replacing the 3P_1 meson a_1 in (a)-(h) with the 1P_1 meson b_1 , one will obtain the corresponding Feynman diagrams for $B \rightarrow b_1 b_1$ decay modes.

where the superscript σ denotes the helicity states of two mesons with $L(T)$ standing for the longitudinal (transverse) component. And the definitions of the amplitudes $\mathcal{M}_i (i = L, N, T)$ in terms of the Lorentz-invariant amplitudes a , b and c are

$$\begin{aligned} m_B^2 \mathcal{M}_L &= a \epsilon_2^*(L) \cdot \epsilon_3^*(L) + \frac{b}{m_{a_1} m_{a_1}} \epsilon_2^*(L) \cdot P_3 \epsilon_3^*(L) \cdot P_2, \\ m_B^2 \mathcal{M}_N &= a, \\ m_B^2 \mathcal{M}_T &= \frac{c}{r_2 r_3}. \end{aligned} \quad (24)$$

We therefore will evaluate the helicity amplitudes $\mathcal{M}_L, \mathcal{M}_N, \mathcal{M}_T$ based on the pQCD approach, respectively.

As illustrated in Fig. 1, there are 8 types of diagrams contributing to the $B \rightarrow a_1 a_1$ and $b_1 b_1$ decays at the lowest order in the pQCD approach. We firstly calculate the usual factorizable spectator(fs) diagrams (a) and (b), in which one can factor out the form factors $B \rightarrow a_1$ and $B \rightarrow b_1$. The corresponding Feynman amplitudes with longitudinal polarization(L) are given as follows,

(i) $(V - A)(V - A)$ operators:

$$\begin{aligned} F_{fs}^L &= 8\pi C_F f_{a_1} m_B^2 \int_0^1 dx_1 dx_3 \int_0^\infty b_1 db_1 b_3 db_3 \\ &\times \phi_B(x_1, b_1) \left\{ [(1+x_3)\phi_{a_1}(x_3) + r_{a_1}(1-2x_3)(\phi_{a_1}^s(x_3) + \phi_{a_1}^t(x_3))] \right. \\ &\times h_{fs}(x_1, x_3, b_1, b_3) E_{fs}(t_a) + 2r_{a_1} \phi_{a_1}^s(x_3) h_{fs}(x_3, x_1, b_3, b_1) E_{fs}(t_b) \left. \right\}, \end{aligned} \quad (25)$$

where $C_F = 4/3$ is a color factor. The convolution functions E_i , the factorization hard scales t_i , and the hard functions h_i can be referred to Ref. [35].

(ii) $(V - A)(V + A)$ operators:

$$F_{fs}^{L;P1} = -F_{fs}^L, \quad (26)$$

which is originated from $\langle a_1 | V + A | 0 \rangle = -\langle a_1 | V - A | 0 \rangle$.

(iii) $(S - P)(S + P)$ operators:

$$F_{fs}^{L;P2} = 0; \quad (27)$$

because the emitted axial-vector meson can not be produced through a scalar or a pseudoscalar current.

For the nonfactorizable spectator(*nfs*) diagrams 1(c) and 1(d), the corresponding decay amplitudes can be read as

(i) $(V - A)(V - A)$ operators:

$$\begin{aligned} M_{nfs}^L = & \frac{32}{\sqrt{6}} \pi C_F m_B^2 \int_0^1 dx_1 dx_2 dx_3 \int_0^\infty b_1 db_1 b_2 db_2 \phi_B(x_1, b_1) \\ & \times \phi_{a_1}(x_2) \{ [(1 - x_2) \phi_{a_1}(x_3) - r_{a_1} x_3 (\phi_{a_1}^s(x_3) - \phi_{a_1}^t(x_3))] \\ & \times E_{nfs}(t_c) h_{nfs}^c(x_1, x_2, x_3, b_1, b_2) - h_{nfs}^d(x_1, x_2, x_3, b_1, b_2) \\ & \times [(x_2 + x_3) \phi_{a_1}(x_3) - r_{a_1} x_3 (\phi_{a_1}^s(x_3) + \phi_{a_1}^t(x_3))] E_{nfs}(t_d) \} , \end{aligned} \quad (28)$$

(ii) $(V - A)(V + A)$ operators:

$$\begin{aligned} M_{nfs}^{L;P1} = & \frac{32}{\sqrt{6}} \pi C_F m_B^2 \int_0^1 dx_1 dx_2 dx_3 \int_0^\infty b_1 db_1 b_2 db_2 \phi_B(x_1, b_1) \\ & \times r_{a_1} \{ [(1 - x_2) (\phi_{a_1}^s(x_2) + \phi_{a_1}^t(x_2)) \phi_{a_1}(x_3) - r_{a_1} (\phi_{a_1}^s(x_2) \\ & \times [(x_2 - x_3 - 1) \phi_{a_1}^s(x_3) - (x_2 + x_3 - 1) \phi_{a_1}^t(x_3)] + \phi_{a_1}^t(x_2) \\ & \times [(x_2 + x_3 - 1) \phi_{a_1}^s(x_3) + (1 - x_2 + x_3) \phi_{a_1}^t(x_3)])] h_{nfs}^c(x_1, x_2, x_3, b_1, b_2) \\ & \times E_{nfs}(t_c) - h_{nfs}^d(x_1, x_2, x_3, b_1, b_2) E_{nfs}(t_d) [x_2 (\phi_{a_1}^s(x_2) - \phi_{a_1}^t(x_2)) \\ & \times \phi_{a_1}(x_3) + r_{a_1} (x_2 (\phi_{a_1}^s(x_2) - \phi_{a_1}^t(x_2)) (\phi_{a_1}^s(x_3) - \phi_{a_1}^t(x_3)) \\ & + x_3 (\phi_{a_1}^s(x_2) + \phi_{a_1}^t(x_2)) (\phi_{a_1}^s(x_3) + \phi_{a_1}^t(x_3)))] \} , \end{aligned} \quad (29)$$

(iii) $(S - P)(S + P)$ operators:

$$\begin{aligned} M_{nfs}^{L;P2} = & \frac{32}{\sqrt{6}} \pi C_F m_B^2 \int_0^1 dx_1 dx_2 dx_3 \int_0^\infty b_1 db_1 b_2 db_2 \phi_B(x_1, b_1) \\ & \times \phi_{a_1}(x_2) \{ [(x_2 - x_3 - 1) \phi_{a_1}(x_3) + r_{a_1} x_3 (\phi_{a_1}^s(x_3) + \phi_{a_1}^t(x_3))] \\ & \times E_{nfs}(t_c) h_{nfs}^c(x_1, x_2, x_3, b_1, b_2) + h_{nfs}^d(x_1, x_2, x_3, b_1, b_2) \\ & \times [x_2 \phi_{a_1}(x_3) - r_{a_1} x_3 (\phi_{a_1}^s(x_3) - \phi_{a_1}^t(x_3))] E_{nfs}(t_d) \} ; \end{aligned} \quad (30)$$

In the above three formulas, i.e., Eqs. (28)-(30), one can find that there exist cancellations between the contributions of the two diagrams in Fig. 1(c) and 1(d).

The Feynman diagrams shown in Fig. 1(e) and 1(f) are the nonfactorizable annihilation(nfa) ones, whose contributions are

(i) $(V - A)(V - A)$ operators:

$$\begin{aligned}
M_{nfa}^L = & \frac{32}{\sqrt{6}} \pi C_F m_B^2 \int_0^1 dx_1 dx_2 dx_3 \int_0^\infty b_1 db_1 b_2 db_2 \\
& \times \phi_B(x_1, b_1) \left\{ \left[(1 - x_3) \phi_{a_1}(x_2) \phi_{a_1}(x_3) + r_{a_1} r_{a_1} (\phi_{a_1}^s(x_2) \right. \right. \\
& \times [(1 + x_2 - x_3) \phi_{a_1}^s(x_3) - (1 - x_2 - x_3) \phi_{a_1}^t(x_3)] + \phi_{a_1}^t(x_2) \\
& \times [(1 - x_2 - x_3) \phi_{a_1}^s(x_3) - (1 + x_2 - x_3) \phi_{a_1}^t(x_3)]) \left. \right] E_{nfa}(t_e) \\
& \times h_{nfa}^e(x_1, x_2, x_3, b_1, b_2) - E_{nfa}(t_f) h_{nfa}^f(x_1, x_2, x_3, b_1, b_2) \\
& \times [x_2 \phi_{a_1}(x_2) \phi_{a_1}(x_3) + r_{a_1} r_{a_1} (\phi_{a_1}^s(x_2) [(x_2 - x_3 + 3) \phi_{a_1}^s(x_3) \\
& + (1 - x_2 - x_3) \phi_{a_1}^t(x_3)] + \phi_{a_1}^t(x_2) [(x_2 + x_3 - 1) \phi_{a_1}^s(x_3) \\
& + (1 - x_2 + x_3) \phi_{a_1}^t(x_3)]) \left. \right] \Big\} , \tag{31}
\end{aligned}$$

(ii) $(V - A)(V + A)$ operators:

$$\begin{aligned}
M_{nfa}^{L;P1} = & \frac{32}{\sqrt{6}} \pi C_F m_B^2 \int_0^1 dx_1 dx_2 dx_3 \int_0^\infty b_1 db_1 b_2 db_2 \\
& \times \phi_B(x_1, b_1) \left\{ \left[r_{a_1} x_2 (\phi_{a_1}^s(x_2) + \phi_{a_1}^t(x_2)) \phi_{a_1}(x_3) - r_{a_1} (1 - x_3) \right. \right. \\
& \times \phi_{a_1}(x_2) (\phi_{a_1}^s(x_3) - \phi_{a_1}^t(x_3)) \left. \right] E_{nfa}(t_e) h_{nfa}^e(x_1, x_2, x_3, b_1, b_2) \\
& + \left[r_{a_1} (2 - x_2) (\phi_{a_1}^s(x_2) + \phi_{a_1}^t(x_2)) \phi_{a_1}(x_3) - r_{a_1} (1 + x_3) \right. \\
& \times \phi_{a_1}(x_2) (\phi_{a_1}^s(x_3) - \phi_{a_1}^t(x_3)) \left. \right] E_{nfa}(t_f) h_{nfa}^f(x_1, x_2, x_3, b_1, b_2) \Big\} , \tag{32}
\end{aligned}$$

(iii) $(S - P)(S + P)$ operators:

$$\begin{aligned}
M_{nfa}^{L;P2} = & -\frac{32}{\sqrt{6}} \pi C_F m_B^2 \int_0^1 dx_1 dx_2 dx_3 \int_0^\infty b_1 db_1 b_2 db_2 \\
& \times \phi_B(x_1, b_1) \left\{ \left[(1 - x_3) \phi_{a_1}(x_2) \phi_{a_1}(x_3) + r_{a_1} r_{a_1} (\phi_{a_1}^s(x_2) \right. \right. \\
& \times [(x_2 - x_3 + 3) \phi_{a_1}^s(x_3) - (1 - x_2 - x_3) \phi_{a_1}^t(x_3)] + \phi_{a_1}^t(x_2) \\
& \times [(1 - x_2 - x_3) \phi_{a_1}^s(x_3) + (1 - x_2 + x_3) \phi_{a_1}^t(x_3)]) \left. \right] E_{nfa}(t_f) \\
& \times h_{nfa}^f(x_1, x_2, x_3, b_1, b_2) - E_{nfa}(t_e) h_{nfa}^e(x_1, x_2, x_3, b_1, b_2) \\
& \times [x_2 \phi_{a_1}(x_2) \phi_{a_1}(x_3) + r_{a_1} r_{a_1} (\phi_{a_1}^s(x_2) [(1 + x_2 - x_3) \phi_{a_1}^s(x_3) \\
& + (1 - x_2 - x_3) \phi_{a_1}^t(x_3)] + \phi_{a_1}^t(x_2) [(x_2 + x_3 - 1) \phi_{a_1}^s(x_3) \\
& - (1 + x_2 - x_3) \phi_{a_1}^t(x_3)]) \left. \right] \Big\} ; \tag{33}
\end{aligned}$$

For the last two diagrams in Fig. 1, i.e., the factorizable annihilation(fa) diagrams 1(g) and 1(h), we have

(i) $(V - A)(V - A)$ operators:

$$\begin{aligned}
F_{fa}^L = & -8\pi C_F m_B^2 \int_0^1 dx_2 dx_3 \int_0^\infty b_2 db_2 b_3 db_3 \{ [x_2 \phi_{a_1}(x_2) \phi_{a_1}(x_3) + 2r_{a_1} r_{a_1} \\
& \times ((x_2 + 1) \phi_{a_1}^s(x_2) + (x_2 - 1) \phi_{a_1}^t(x_2)) \phi_{a_1}^s(x_3)] h_{fa}(x_2, 1 - x_3, b_2, b_3) \\
& \times E_{fa}(t_g) - [(1 - x_3) \phi_{a_1}(x_2) \phi_{a_1}(x_3) - 2r_{a_1} r_{a_1} \phi_{a_1}^s(x_2) ((x_3 - 2) \phi_{a_1}^s(x_3) \\
& - x_3 \phi_{a_1}^t(x_3))] E_{fa}(t_h) h_{fa}(1 - x_3, x_2, b_3, b_2) \} , \quad (34)
\end{aligned}$$

(ii) $(V - A)(V + A)$ operators:

$$F_{fa}^{L;P1} = F_{fa}^L , \quad (35)$$

(iii) $(S - P)(S + P)$ operators:

$$\begin{aligned}
F_{fa}^{L;P2} = & 16\pi C_F m_B^2 \int_0^1 dx_2 dx_3 \int_0^\infty b_2 db_2 b_3 db_3 \{ [2r_{a_1} \phi_{a_1}(x_2) \phi_{a_1}^s(x_3) \\
& + r_{a_1} x_2 (\phi_{a_1}^s(x_2) - \phi_{a_1}^t(x_2)) \phi_{a_1}(x_3)] h_{fa}(x_2, 1 - x_3, b_2, b_3) E_{fa}(t_g) \\
& + [2r_{a_1} \phi_{a_1}^s(x_2) \phi_{a_1}(x_3) + r_{a_1} (1 - x_3) \phi_{a_1}(x_2) (\phi_{a_1}^s(x_3) + \phi_{a_1}^t(x_3))] \\
& \times E_{fa}(t_h) h_{fa}(1 - x_3, x_2, b_3, b_2) \} . \quad (36)
\end{aligned}$$

It is interesting to notice that there is a large cancellation in the F_{fa}^L , i.e., Eq. (34), from the factorizable annihilation diagrams 1(g) and 1(h), which can result in the exact zero contribution in the SU(3) limit.

We can also present the factorization formulas for the Feynman amplitudes with transverse polarizations,

$$\begin{aligned}
F_{fs}^N = & 8\pi C_F f_{a_1} m_B^2 \int_0^1 dx_1 dx_3 \int_0^\infty b_1 db_1 b_3 db_3 \phi_B(x_1, b_1) r_{a_1} \\
& \times \{ [\phi_{a_1}^T(x_3) + r_{a_1} x_3 (\phi_{a_1}^v(x_3) - \phi_{a_1}^a(x_3)) + 2r_{a_1} \phi_{a_1}^v(x_3)] E_{fs}(t_a) \\
& \times h_{fs}(x_1, x_3, b_1, b_3) + r_{a_1} (\phi_{a_1}^a(x_3) + \phi_{a_1}^v(x_3)) h_{fs}(x_3, x_1, b_3, b_1) E_{fs}(t_b) \} , \quad (37)
\end{aligned}$$

$$\begin{aligned}
F_{fs}^T = & 16\pi C_F f_{a_1} m_B^2 \int_0^1 dx_1 dx_3 \int_0^\infty b_1 db_1 b_3 db_3 \phi_B(x_1, b_1) r_{a_1} \\
& \times \{ [\phi_{a_1}^T(x_3) - r_{a_1} x_3 (\phi_{a_1}^v(x_3) - \phi_{a_1}^a(x_3)) + 2r_{a_1} \phi_{a_1}^a(x_3)] E_{fs}(t_a) \\
& \times h_{fs}(x_1, x_3, b_1, b_3) + r_{a_1} (\phi_{a_1}^a(x_3) + \phi_{a_1}^v(x_3)) h_{fs}(x_3, x_1, b_3, b_1) E_{fs}(t_b) \} , \quad (38)
\end{aligned}$$

$$F_{fs}^{N;P1} = -F_{fs}^N , \quad (39)$$

$$F_{fs}^{T;P1} = -F_{fs}^T ; \quad (40)$$

$$F_{fs}^{N;P2} = 0 , \quad (41)$$

$$F_{fs}^{T;P2} = 0 ; \quad (42)$$

$$\begin{aligned}
M_{nfs}^N &= \frac{32}{\sqrt{6}} \pi C_F m_B^2 \int_0^1 dx_1 dx_2 dx_3 \int_0^\infty b_1 db_1 b_2 db_2 \phi_B(x_1, b_1) r_{a_1} \\
&\times \left\{ [(1-x_2)(\phi_{a_1}^a(x_2) + \phi_{a_1}^v(x_2))\phi_{a_1}^T(x_3)] h_{nfs}^c(x_1, x_2, x_3, b_1, b_2) \right. \\
&\times E_{nfs}(t_c) + h_{nfs}^d(x_1, x_2, x_3, b_1, b_2) [x_2(\phi_{a_1}^a(x_2) + \phi_{a_1}^v(x_2))\phi_{a_1}^T(x_3) \\
&\left. - 2r_{a_1}(x_2 + x_3)(\phi_{a_1}^a(x_2)\phi_{a_1}^a(x_3) + \phi_{a_1}^v(x_2)\phi_{a_1}^v(x_3))] E_{nfs}(t_d) \right\} , \quad (43)
\end{aligned}$$

$$\begin{aligned}
M_{nfs}^T &= \frac{64}{\sqrt{6}} \pi C_F m_B^2 \int_0^1 dx_1 dx_2 dx_3 \int_0^\infty b_1 db_1 b_2 db_2 \phi_B(x_1, b_1) r_{a_1} \\
&\times \left\{ [(1-x_2)(\phi_{a_1}^a(x_2) + \phi_{a_1}^v(x_2))\phi_{a_1}^T(x_3)] h_{nfs}^c(x_1, x_2, x_3, b_1, b_2) \right. \\
&\times E_{nfs}(t_c) + h_{nfs}^d(x_1, x_2, x_3, b_1, b_2) [x_2(\phi_{a_1}^a(x_2) + \phi_{a_1}^v(x_2))\phi_{a_1}^T(x_3) \\
&\left. - 2r_{a_1}(x_2 + x_3)(\phi_{a_1}^v(x_2)\phi_{a_1}^a(x_3) + \phi_{a_1}^a(x_2)\phi_{a_1}^v(x_3))] E_{nfs}(t_d) \right\} , \quad (44)
\end{aligned}$$

$$\begin{aligned}
M_{nfs}^{N;P_1} &= -\frac{32}{\sqrt{6}} \pi C_F m_B^2 \int_0^1 dx_1 dx_2 dx_3 \int_0^\infty b_1 db_1 b_2 db_2 \phi_B(x_1, b_1) r_{a_1} \\
&\times x_3 \phi_{a_1}^T(x_2)(\phi_{a_1}^a(x_3) - \phi_{a_1}^v(x_3)) [h_{nfs}^c(x_1, x_2, x_3, b_1, b_2) E_{nfs}(t_c) \\
&+ h_{nfs}^d(x_1, x_2, x_3, b_1, b_2) E_{nfs}(t_d)] , \quad (45)
\end{aligned}$$

$$M_{nfs}^{T;P_1} = 2 M_{nfs}^{N;P_1} ; \quad (46)$$

$$\begin{aligned}
M_{nfs}^{N;P_2} &= -\frac{32}{\sqrt{6}} \pi C_F m_B^2 \int_0^1 dx_1 dx_2 dx_3 \int_0^\infty b_1 db_1 b_2 db_2 \phi_B(x_1, b_1) r_{a_1} \\
&\times \left\{ [x_2(\phi_{a_1}^a(x_2) - \phi_{a_1}^v(x_2))\phi_{a_1}^T(x_3)] h_{nfs}^d(x_1, x_2, x_3, b_1, b_2) \right. \\
&\times E_{nfs}(t_d) + h_{nfs}^c(x_1, x_2, x_3, b_1, b_2) [x_2(\phi_{a_1}^a(x_2) - \phi_{a_1}^v(x_2))\phi_{a_1}^T(x_3) \\
&\left. + 2r_{a_1}(1 - x_2 + x_3)(\phi_{a_1}^v(x_2)\phi_{a_1}^v(x_3) - \phi_{a_1}^a(x_2)\phi_{a_1}^a(x_3))] E_{nfs}(t_c) \right\} , \quad (47)
\end{aligned}$$

$$\begin{aligned}
M_{nfs}^{T;P_2} &= -\frac{64}{\sqrt{6}} \pi C_F m_B^2 \int_0^1 dx_1 dx_2 dx_3 \int_0^\infty b_1 db_1 b_2 db_2 \phi_B(x_1, b_1) r_{a_1} \\
&\times \left\{ [x_2(\phi_{a_1}^a(x_2) - \phi_{a_1}^v(x_2))\phi_{a_1}^T(x_3)] h_{nfs}^d(x_1, x_2, x_3, b_1, b_2) \right. \\
&\times E_{nfs}(t_d) + h_{nfs}^c(x_1, x_2, x_3, b_1, b_2) [x_2(\phi_{a_1}^a(x_2) - \phi_{a_1}^v(x_2))\phi_{a_1}^T(x_3) \\
&\left. + 2r_{a_1}(1 - x_2 + x_3)(\phi_{a_1}^v(x_2)\phi_{a_1}^a(x_3) - \phi_{a_1}^a(x_2)\phi_{a_1}^v(x_3))] E_{nfs}(t_c) \right\} , \quad (48)
\end{aligned}$$

$$\begin{aligned}
M_{nfa}^N &= -\frac{64}{\sqrt{6}} \pi C_F m_B^2 \int_0^1 dx_1 dx_2 dx_3 \int_0^\infty b_1 db_1 b_2 db_2 r_{a_1} r_{a_1} \\
&\times \phi_B(x_1, b_1) \left\{ h_{nfa}^f(x_1, x_2, x_3, b_1, b_2) E_{nfa}(t_f) \right. \\
&\times [\phi_{a_1}^a(x_2)\phi_{a_1}^a(x_3) + \phi_{a_1}^v(x_2)\phi_{a_1}^v(x_3)] \left. \right\} , \quad (49)
\end{aligned}$$

$$\begin{aligned}
M_{nfa}^T &= -\frac{128}{\sqrt{6}} \pi C_F m_B^2 \int_0^1 dx_1 dx_2 dx_3 \int_0^\infty b_1 db_1 b_2 db_2 r_{a_1} r_{a_1} \\
&\times \phi_B(x_1, b_1) \left\{ h_{nfa}^f(x_1, x_2, x_3, b_1, b_2) E_{nfa}(t_f) \right. \\
&\times [\phi_{a_1}^v(x_2)\phi_{a_1}^a(x_3) + \phi_{a_1}^a(x_2)\phi_{a_1}^v(x_3)] \left. \right\} , \quad (50)
\end{aligned}$$

$$\begin{aligned}
M_{nfa}^{N;P_1} = & \frac{32}{\sqrt{6}} \pi C_F m_B^2 \int_0^1 dx_1 dx_2 dx_3 \int_0^\infty b_1 db_1 b_2 db_2 \\
& \times \phi_B(x_1, b_1) \left\{ \left[r_{a_1} x_2 (\phi_{a_1}^a(x_2) + \phi_{a_1}^v(x_2)) \phi_{a_1}^T(x_3) - r_{a_1} (1 - x_3) \right. \right. \\
& \times \phi_{a_1}^T(x_2) (\phi_{a_1}^a(x_3) - \phi_{a_1}^v(x_3)) \left. \right] E_{nfa}(t_e) h_{nfa}^e(x_1, x_2, x_3, b_1, b_2) \\
& + \left[r_{a_1} (2 - x_2) (\phi_{a_1}^a(x_2) + \phi_{a_1}^v(x_2)) \phi_{a_1}^T(x_3) - r_{a_1} (1 + x_3) \right. \\
& \times \phi_{a_1}^T(x_2) (\phi_{a_1}^a(x_3) - \phi_{a_1}^v(x_3)) \left. \right] E_{nfa}(t_f) h_{nfa}^f(x_1, x_2, x_3, b_1, b_2) \left. \right\} , \quad (51)
\end{aligned}$$

$$M_{nfa}^{T;P_1} = 2 M_{nfa}^{N;P_1} ; \quad (52)$$

$$M_{nfa}^{N;P_2} = M_{nfa}^N , \quad (53)$$

$$M_{nfa}^{T;P_2} = -M_{nfa}^T ; \quad (54)$$

$$\begin{aligned}
F_{fa}^N = & 8\pi C_F m_B^2 \int_0^1 dx_2 dx_3 \int_0^\infty b_2 db_2 b_3 db_3 r_{a_1} r_{a_1} \left\{ \left[\phi_{a_1}^a(x_2) ((x_2 + 1) \phi_{a_1}^a(x_3) \right. \right. \\
& + (x_2 - 1) \phi_{a_1}^v(x_3)) + \phi_{a_1}^v(x_2) ((x_2 + 1) \phi_{a_1}^v(x_3) + (x_2 - 1) \phi_{a_1}^a(x_3)) \left. \right] E_{fa}(t_g) \\
& \times h_{fa}(x_2, 1 - x_3, b_2, b_3) + \left[(x_3 - 2) (\phi_{a_1}^a(x_2) \phi_{a_1}^a(x_3) + \phi_{a_1}^v(x_2) \phi_{a_1}^v(x_3)) \right. \\
& \left. \left. - x_3 (\phi_{a_1}^a(x_2) \phi_{a_1}^v(x_3) + \phi_{a_1}^v(x_2) \phi_{a_1}^a(x_3)) \right] E_{fa}(t_h) h_{fa}(1 - x_3, x_2, b_3, b_2) \right\} , \quad (55)
\end{aligned}$$

$$\begin{aligned}
F_{fa}^T = & 16\pi C_F m_B^2 \int_0^1 dx_2 dx_3 \int_0^\infty b_2 db_2 b_3 db_3 r_{a_1} r_{a_1} \left\{ \left[\phi_{a_1}^v(x_2) ((x_2 + 1) \phi_{a_1}^a(x_3) \right. \right. \\
& + (x_2 - 1) \phi_{a_1}^v(x_3)) + \phi_{a_1}^a(x_2) ((x_2 + 1) \phi_{a_1}^v(x_3) + (x_2 - 1) \phi_{a_1}^a(x_3)) \left. \right] E_{fa}(t_g) \\
& \times h_{fa}(x_2, 1 - x_3, b_2, b_3) + \left[(x_3 - 2) (\phi_{a_1}^a(x_2) \phi_{a_1}^v(x_3) + \phi_{a_1}^v(x_2) \phi_{a_1}^a(x_3)) \right. \\
& \left. \left. - x_3 (\phi_{a_1}^a(x_2) \phi_{a_1}^a(x_3) + \phi_{a_1}^v(x_2) \phi_{a_1}^v(x_3)) \right] E_{fa}(t_h) h_{fa}(1 - x_3, x_2, b_3, b_2) \right\} , \quad (56)
\end{aligned}$$

$$F_{fa}^{N;P_1} = F_{fa}^N , \quad (57)$$

$$F_{fa}^{T;P_1} = F_{fa}^T , \quad (58)$$

$$\begin{aligned}
F_{fa}^{N;P_2} = & 16\pi C_F m_B^2 \int_0^1 dx_2 dx_3 \int_0^\infty b_2 db_2 b_3 db_3 r_{a_1} \\
& \times \left\{ \left[\phi_{a_1}^T(x_2) (\phi_{a_1}^a(x_3) - \phi_{a_1}^v(x_3)) \right] E_{fa}(t_g) h_{fa}(x_2, 1 - x_3, b_2, b_3) \right. \\
& \left. + \left[(\phi_{a_1}^a(x_2) + \phi_{a_1}^v(x_2)) \phi_{a_1}^T(x_3) \right] E_{fa}(t_h) h_{fa}(1 - x_3, x_2, b_3, b_2) \right\} , \quad (59)
\end{aligned}$$

$$F_{fa}^{T;P_2} = 2 F_{fa}^{N;P_2} . \quad (60)$$

Thus, for these considered six tree-dominated decay channels, by combining all the possible contributions from different Feynman diagrams, we can display the physical decay

amplitudes with three polarizations $h = L, N, T$ as follows,

$$\begin{aligned} \mathcal{M}_h(B^0 \rightarrow a_1^+ a_1^-) = & \lambda_u \left[a_1 F_{fs}^h + C_1 M_{nfs}^h + C_2 M_{nfa}^h + a_2 f_B F_{fa}^h \right] - \lambda_t \left[(a_4 + a_{10}) F_{fs}^h \right. \\ & + (C_3 + C_9) M_{nfs}^h + (C_5 + C_7) M_{nfs}^{h;P_1} + (C_3 + 2C_4 - \frac{1}{2}(C_9 - C_{10})) \\ & \times M_{nfa}^h + (C_5 - \frac{1}{2}C_7) M_{nfa}^{h;P_1} + (2C_6 + \frac{1}{2}C_8) M_{nfa}^{h;P_2} + (2a_3 + a_4 \\ & \left. + 2a_5 + \frac{1}{2}(a_7 + a_9 - a_{10})) f_B F_{fa}^h + (a_6 - \frac{1}{2}a_8) f_B F_{fa}^{h;P_2} \right], \end{aligned} \quad (61)$$

$$\begin{aligned} \sqrt{2} \mathcal{M}_h(B^+ \rightarrow a_1^+ a_1^0) = & \lambda_u \left[(a_1 + a_2) F_{fs}^h + (C_1 + C_2) M_{nfs}^h \right] - \lambda_t \left[(2(C_9 + C_{10}) \right. \\ & - \frac{1}{2}(3C_7 + C_8)) F_{fs}^h + \frac{3}{2}(C_9 + C_{10}) M_{nfs}^h + \frac{3}{2}C_7 M_{nfs}^{h;P_1} \\ & \left. + \frac{3}{2}C_8 M_{nfs}^{h;P_2} \right], \end{aligned} \quad (62)$$

$$\begin{aligned} \sqrt{2} \mathcal{M}_h(B^0 \rightarrow a_1^0 a_1^0) = & \lambda_u \left[a_2 (f_B F_{fa}^h - F_{fs}^h) + C_2 (M_{nfa}^h - M_{nfs}^h) \right] - \lambda_t \left[(a_4 - \frac{1}{2}(3a_7 \right. \\ & + 3a_9 + a_{10})) F_{fs}^h + (C_3 - \frac{1}{2}(C_9 + 3C_{10})) M_{nfs}^h - (C_5 - \frac{1}{2}C_7) \\ & \times M_{nfs}^{h;P_1} - \frac{3}{2}C_8 M_{nfs}^{h;P_2} + (C_3 + 2C_4 - \frac{1}{2}(C_9 - C_{10})) M_{nfa}^h \\ & + (C_5 - \frac{1}{2}C_7) M_{nfa}^{h;P_1} + (2C_6 + \frac{1}{2}C_8) M_{nfa}^{h;P_2} + (2a_3 + a_4 + 2a_5 \\ & \left. + \frac{1}{2}(a_7 - a_9 + a_{10})) f_B F_{fa}^h + (a_6 - \frac{1}{2}a_8) f_B F_{fa}^{h;P_2} \right]. \end{aligned} \quad (63)$$

In the above Eqs. (61)-(63), λ_u and λ_t stand for the products of CKM matrix elements $V_{ub}^* V_{ud}$ and $V_{tb}^* V_{td}$, respectively. The standard combinations a_i (r.h.s.) of Wilson coefficients are defined as follows,

$$a_1 = C_2 + \frac{C_1}{3}, \quad a_2 = C_1 + \frac{C_2}{3}, \quad a_i = C_i + \frac{C_{i\pm 1}}{3} (i = 3 - 10). \quad (64)$$

where the upper(lower) sign applies, when i is odd(even). While for $B \rightarrow b_1 b_1$ decay channels, one can easily obtain the analytic formulas for various decay amplitudes just by replacing a_1 with b_1 in Eqs. (25)-(63) correspondingly.

IV. NUMERICAL RESULTS AND DISCUSSIONS

In this section, we will calculate numerically the CP-averaged BRs, polarization fractions, direct CP-violating asymmetries, and relative phases for those considered $B \rightarrow a_1 a_1$ and $b_1 b_1$ decay modes. In numerical calculations, central values of the input parameters will be used implicitly unless otherwise stated.

TABLE I. The CP-averaged predictions of physical observables for $B^0 \rightarrow a_1^+ a_1^-$, $b_1^+ b_1^-$ decays obtained in the pQCD approach(This work). For comparison, we also cite the available experimental measurements [5] and the theoretical estimates in the framework of QCD factorization [3].

Decay Channels		$B^0 \rightarrow a_1^+ a_1^-$			$B^0 \rightarrow b_1^+ b_1^-$		
Parameter	Definition	This work	QCDF	Experiment	This work	QCDF	Experiment
BR(10^{-6})	$\Gamma/\Gamma_{\text{total}}$	$54.7^{+19.4+29.4+5.7}_{-16.9-23.2-4.4}$	$37.4^{+16.1+9.7}_{-13.7-1.4}$	$47.3^{+10.5+6.3}_{-10.5-6.3}$	$21.4^{+5.7+18.1+2.1}_{-5.3-11.3-1.4}$	$1.0^{+1.6+15.7}_{-0.7-0.3}$	—
f_L	$ \mathcal{A}_L ^2$	$0.76^{+0.01+0.03+0.00}_{-0.00-0.04-0.00}$	$0.64^{+0.07}_{-0.17}$	$0.31^{+0.22+0.10}_{-0.22-0.10}$	$0.88^{+0.02+0.04+0.01}_{-0.01-0.05-0.00}$	$0.96^{+0.03}_{-0.65}$	—
$f_{ }$	$ \mathcal{A}_{ } ^2$	$0.14^{+0.00+0.02+0.00}_{-0.00-0.02-0.00}$	—	—	$0.07^{+0.01+0.03+0.00}_{-0.01-0.02-0.00}$	—	—
f_{\perp}	$ \mathcal{A}_{\perp} ^2$	$0.10^{+0.00+0.02+0.00}_{-0.00-0.01-0.00}$	—	—	$0.05^{+0.01+0.02+0.00}_{-0.01-0.01-0.00}$	—	—
$\phi_{ }(\text{rad})$	$\pi + \arg \frac{\mathcal{A}_{ }}{\mathcal{A}_L}$	$3.16^{+0.01+0.06+0.01}_{-0.01-0.04-0.01}$	—	—	$2.51^{+0.07+0.07+0.01}_{-0.06-0.06-0.01}$	—	—
$\phi_{\perp}(\text{rad})$	$\pi + \arg \frac{\mathcal{A}_{\perp}}{\mathcal{A}_L}$	$3.17^{+0.01+0.06+0.03}_{-0.00-0.04-0.01}$	—	—	$2.47^{+0.06+0.08+0.01}_{-0.05-0.08-0.01}$	—	—
$\Delta\phi_{ }(\text{rad})$	$\frac{\phi_{ }-\phi_{ }}{2}$	$-0.04^{+0.00+0.01+0.00}_{-0.01-0.01-0.01}$	—	—	$0.43^{+0.02+0.07+0.02}_{-0.04-0.09-0.04}$	—	—
$\Delta\phi_{\perp}(\text{rad})$	$\frac{\phi_{\perp}-\phi_{\perp}-\pi}{2}$	$-1.62^{+0.01+0.01+0.00}_{-0.01-0.01-0.01}$	—	—	$-1.15^{+0.04+0.09+0.02}_{-0.02-0.09-0.03}$	—	—
$\mathcal{A}_{CP}^{\text{dir}}$	$\frac{\Gamma-\bar{\Gamma}}{\Gamma+\bar{\Gamma}}$	$-0.04^{+0.01+0.01+0.00}_{-0.01-0.01-0.00}$	—	—	$-0.00^{+0.01+0.00+0.00}_{-0.04-0.01-0.00}$	—	—
$\mathcal{A}_{CP}^{\text{dir},L}$	$\frac{f_L-f_L}{f_L+f_L}$	$0.11^{+0.02+0.01+0.00}_{-0.02-0.01-0.01}$	—	—	$-0.05^{+0.04+0.02+0.00}_{-0.04-0.03-0.00}$	—	—
$\mathcal{A}_{CP}^{\text{dir}, }$	$\frac{f_{ }-f_{ }}{f_{ }+f_{ }}$	$-0.52^{+0.08+0.10+0.04}_{-0.07-0.07-0.02}$	—	—	$0.34^{+0.05+0.02+0.01}_{-0.06-0.04-0.03}$	—	—
$\mathcal{A}_{CP}^{\text{dir},\perp}$	$\frac{f_{\perp}-f_{\perp}}{f_{\perp}+f_{\perp}}$	$-0.54^{+0.08+0.11+0.04}_{-0.06-0.06-0.01}$	—	—	$0.38^{+0.06+0.03+0.02}_{-0.06-0.04-0.02}$	—	—

The QCD scale (GeV), masses (GeV), and B meson lifetime(ps) are [14, 36]

$$\Lambda_{\overline{\text{MS}}}^{(f=4)} = 0.250, \quad m_W = 80.41, \quad m_{a_1} = 1.23, \quad m_{b_1} = 1.21; \\ m_B = 5.279, \quad m_b = 4.8, \quad \tau_{B^+} = 1.638, \quad \tau_{B^0} = 1.53. \quad (65)$$

For the CKM matrix elements, we adopt the Wolfenstein parametrization and the updated parameters $A = 0.814$, $\lambda = 0.2257$, $\bar{\rho} = 0.135$, and $\bar{\eta} = 0.349$ [36].

Utilizing the above chosen distribution amplitudes and the central values of the relevant input parameters, the resultant $B \rightarrow a_1$ and $B \rightarrow b_1$ form factors at maximal recoil,

$$V_0^{B \rightarrow a_1} = 0.34^{+0.10}_{-0.09}, \quad A^{B \rightarrow a_1} = 0.27^{+0.06}_{-0.05}, \quad V_1^{B \rightarrow a_1} = 0.41^{+0.10}_{-0.08}; \quad (66)$$

$$V_0^{B \rightarrow b_1} = 0.45^{+0.08}_{-0.09}, \quad A^{B \rightarrow b_1} = 0.20^{+0.05}_{-0.04}, \quad V_1^{B \rightarrow b_1} = 0.30^{+0.07}_{-0.06}. \quad (67)$$

associated with the longitudinal, parallel, and perpendicular components of the $B \rightarrow a_1 a_1$ and $B \rightarrow b_1 b_1$ decays, respectively, are in good consistency with those as given in Ref. [29].

As a comparison, we quote the form factors used in the $B \rightarrow a_1 a_1$ and $b_1 b_1$ decays in the QCD factorization [3],

$$V_0^{B \rightarrow a_1} = 0.30 \pm 0.05, \quad A^{B \rightarrow a_1} = 0.30 \pm 0.05, \quad V_1^{B \rightarrow a_1} = 0.60 \pm 0.11; \quad (68)$$

$$V_0^{B \rightarrow b_1} = 0.39 \pm 0.07, \quad A^{B \rightarrow b_1} = 0.16 \pm 0.03, \quad V_1^{B \rightarrow b_1} = 0.32 \pm 0.06. \quad (69)$$

One can find that the form factors in the light-cone sum rule(LCSR), Eq. (68,69), are basically consistent with those in the pQCD approach, Eq. (66,67), within errors. But, it should be noticed that, for $B \rightarrow a_1$ transition, $V_{0;\text{LCSR}} < V_{0;\text{pQCD}}$ in the longitudinal polarization while $A_{\text{LCSR}} > A_{\text{pQCD}}$ and $V_{1;\text{LCSR}} > V_{1;\text{pQCD}}$ in both tranverse polarizations, which may reduce the polarization fraction f_L , for example, for $B^0 \rightarrow a_1^+ a_1^-$ mode evidently.

A. CP-averaged Branching Ratios

For $B \rightarrow a_1 a_1$ and $b_1 b_1$ decays, the decay rate can be written explicitly as,

$$\Gamma = \frac{G_F^2 |\mathbf{P}_c|}{16\pi m_B^2} \sum_{\sigma=L,T} \mathcal{M}^{(\sigma)\dagger} \mathcal{M}^{(\sigma)} \quad (70)$$

where $|\mathbf{P}_c| \equiv |\mathbf{P}_{2z}| = |\mathbf{P}_{3z}|$ is the momentum of either of the outgoing axial-vector mesons and $\mathcal{M}^{(\sigma)}$ can be found in Eqs. (61)-(63).

The theoretical predictions on CP-averaged BRs for $B \rightarrow a_1 a_1$ and $b_1 b_1$ decays evaluated in the pQCD approach, together with the results in QCDF approach and the available experimental data, have been grouped in Tables I-III. The first error is from the B meson wave function shape parameter $\omega_B = 0.40 \pm 0.04$ GeV and decay constant $f_B = 0.19 \pm 0.02$ GeV. The second and dominant theoretical error in these entries arises from the combination of the uncertainties of Gegenbauer moments $a_{2,a_1}^{\parallel}(a_{1,b_1}^{\parallel})$, $a_{1,a_1}^{\perp}(a_{2,b_1}^{\perp})$, and decay constant $f_{a_1}(f_{b_1})$ in the distribution amplitudes of axial-vector meson $a_1(b_1)$. The third error is also the combined uncertainty in the CKM matrix elements: $\bar{\rho} = 0.135_{-0.016}^{+0.031}$ and $\bar{\eta} = 0.349_{-0.017}^{+0.015}$ [36]. The numerical results implicated that the input parameters (e.g. the Gegenbauer coefficients in the nonperturbative wave functions of involved mesons) adopted in the pQCD approach should be further improved through the better constraints from the experiments to enhance the theoretical precision.

By comparison, one can easily find that the results on the CP-averaged BRs of $B \rightarrow a_1 a_1$ decays in the pQCD approach agree well with those obtained in the QCDF within large theoretical errors,

$$\left. \begin{aligned} \text{BR}(B^0 \rightarrow a_1^+ a_1^-) &= 54.7_{-29.0}^{+35.7} \times 10^{-6}, \\ \text{BR}(B^+ \rightarrow a_1^+ a_1^0) &= 21.4_{-10.5}^{+12.6} \times 10^{-6}, \\ \text{BR}(B^0 \rightarrow a_1^0 a_1^0) &= 2.2_{-1.1}^{+1.7} \times 10^{-6}; \end{aligned} \right\} \quad (\text{In pQCD}) \quad (71)$$

and

$$\left. \begin{aligned} \text{BR}(B^0 \rightarrow a_1^+ a_1^-) &= 37.4_{-13.8}^{+18.8} \times 10^{-6}, \\ \text{BR}(B^+ \rightarrow a_1^+ a_1^0) &= 22.4_{-8.3}^{+12.6} \times 10^{-6}, \\ \text{BR}(B^0 \rightarrow a_1^0 a_1^0) &= 0.5_{-0.2}^{+9.3} \times 10^{-6}. \end{aligned} \right\} \quad (\text{In QCDF}) \quad (72)$$

in which various errors have been added in quadrature.

Based on those numerical results given in Tables I-III, some remarks on the CP-averaged BRs for $B \rightarrow a_1 a_1$ decays are in order:

1. As mentioned in the introduction, the experimental measurement for $B^0 \rightarrow a_1^+ a_1^-$ mode has been performed by BaBar Collaboration and the decay rate is [5, 10],

$$\text{BR}(B^0 \rightarrow a_1^+ a_1^-)_{\text{Exp.}} = 47.3_{-12.2}^{+12.2} \times 10^{-6}. \quad (73)$$

Combined with the numerical results evaluated with pQCD and QCDF approaches², i.e., Eqs. (71) and (72), one can find that the predicted $\text{BR}(B^0 \rightarrow a_1^+ a_1^-)_{\text{Th.}}$ agree well with the present data within uncertainties.

² Here, we do not quote $\text{BR}(B^0 \rightarrow a_1^+ a_1^-)$ provided in naive factorization [2] for phenomenological analysis just because the numerical result is too small to be comparable with the data.

TABLE II. Same as Table I but for $B^+ \rightarrow a_1^+ a_1^0, b_1^+ b_1^0$ decays.

Decay Channels		$B^+ \rightarrow a_1^+ a_1^0$			$B^+ \rightarrow b_1^+ b_1^0$		
Parameter	Definition	This work	QCDF	Experiment	This work	QCDF	Experiment
BR(10^{-6})	$\Gamma/\Gamma_{\text{total}}$	$21.4^{+7.4+10.0+2.2}_{-6.5-8.2-1.0}$	$22.4^{+10.7+6.6}_{-8.2-1.5}$	—	$7.6^{+2.3+6.8+0.8}_{-1.9-4.1-0.6}$	$1.4^{+2.5+2.8}_{-1.0-0.0}$	—
f_L	$ \mathcal{A}_L ^2$	$0.91^{+0.00+0.02+0.00}_{-0.00-0.03-0.00}$	$0.74^{+0.24}_{-0.32}$	—	$0.84^{+0.01+0.05+0.00}_{-0.01-0.08-0.00}$	$0.95^{+0.00}_{-0.82}$	—
$f_{ }$	$ \mathcal{A}_{ } ^2$	$0.05^{+0.00+0.02+0.00}_{-0.00-0.01-0.00}$	—	—	$0.10^{+0.00+0.04+0.00}_{-0.01-0.03-0.00}$	—	—
f_{\perp}	$ \mathcal{A}_{\perp} ^2$	$0.03^{+0.01+0.02+0.00}_{-0.00-0.00-0.00}$	—	—	$0.07^{+0.00+0.03+0.00}_{-0.01-0.02-0.00}$	—	—
$\phi_{ }(\text{rad})$	$\pi + \arg \frac{\mathcal{A}_{ }}{\mathcal{A}_L}$	$3.28^{+0.02+0.08+0.00}_{-0.02-0.09-0.00}$	—	—	$2.75^{+0.06+0.06+0.00}_{-0.05-0.05-0.00}$	—	—
$\phi_{\perp}(\text{rad})$	$\pi + \arg \frac{\mathcal{A}_{\perp}}{\mathcal{A}_L}$	$3.28^{+0.02+0.09+0.00}_{-0.02-0.10-0.00}$	—	—	$2.77^{+0.06+0.07+0.00}_{-0.05-0.05-0.00}$	—	—
$\Delta\phi_{ }(\text{rad})$	$\frac{\bar{\phi}_{ }-\phi_{ }}{2}$	≈ 0.0	—	—	≈ 0.0	—	—
$\Delta\phi_{\perp}(\text{rad})$	$\frac{\bar{\phi}_{\perp}-\phi_{\perp}-\pi}{2}$	≈ -1.58	—	—	≈ -1.57	—	—
$\mathcal{A}_{CP}^{\text{dir}}$	$\frac{\bar{\Gamma}-\Gamma}{\bar{\Gamma}+\Gamma}$	≈ 0.0	—	—	≈ 0.0	—	—
$\mathcal{A}_{CP}^{\text{dir},L}$	$\frac{\bar{f}_L-f_L}{\bar{f}_L+f_L}$	≈ 0.0	—	—	≈ 0.0	—	—
$\mathcal{A}_{CP}^{\text{dir}, }$	$\frac{\bar{f}_{ }-f_{ }}{\bar{f}_{ }+f_{ }}$	≈ 0.0	—	—	≈ 0.0	—	—
$\mathcal{A}_{CP}^{\text{dir},\perp}$	$\frac{\bar{f}_{\perp}-f_{\perp}}{\bar{f}_{\perp}+f_{\perp}}$	≈ 0.0	—	—	≈ 0.0	—	—

- Based on the discussions [3, 8, 9] about the hadron dynamics of axial-vector a_1 and vector ρ mesons, due to the similar QCD behavior between them, the decay pattern of $B \rightarrow a_1 a_1$ modes is therefore analogous to that of $B \rightarrow \rho \rho$ ones as expected.
- Because the decay constant $f_{a_1} \approx 1.2 \times f_{\rho} \approx 1.5 \times f_{\rho}^T$, the pattern of $\text{BR}(B \rightarrow a_1 a_1) > \text{BR}(B \rightarrow \rho \rho)$ is also as expected in the pQCD approach correspondingly. But, it is worth mentioning that for the color-suppressed decay $B^0 \rightarrow a_1^0 a_1^0$, $\text{BR}(B^0 \rightarrow a_1^0 a_1^0)_{\text{pQCD}} \approx 4 \times \text{BR}(B^0 \rightarrow a_1^0 a_1^0)_{\text{QCDF}}$.
- Actually, in view of the larger decay constant f_{a_1} and similar QCD behavior of a_1 to ρ , as a naive estimate, the relation of the BRs among three channels $B^0 \rightarrow \rho^0 \rho^0$, $B^0 \rightarrow a_1^0 \rho^0$, and $B^0 \rightarrow a_1^0 a_1^0$ may be $\text{BR}(B^0 \rightarrow \rho^0 \rho^0) < \text{BR}(B^0 \rightarrow a_1^0 \rho^0) < \text{BR}(B^0 \rightarrow a_1^0 a_1^0)$. In other words, $\text{BR}(B^0 \rightarrow a_1^0 a_1^0)_{\text{QCDF}}$ should be comparable with $\text{BR}(B^0 \rightarrow a_1^0 a_1^0)_{\text{pQCD}}$. It is thus a bit strange that $\text{BR}(B^0 \rightarrow \rho^0 \rho^0) \approx 2 \times \text{BR}(B^0 \rightarrow a_1^0 a_1^0)$ and $\text{BR}(B^0 \rightarrow a_1^0 \rho^0) \approx 2.5 \times \text{BR}(B^0 \rightarrow a_1^0 a_1^0)$ in Ref. [3] within the framework of QCDF. It is worth stressing that among the above comparisons, the central values of the theoretical predictions are adopted for clarification.
- Similar to $B \rightarrow \pi \pi$ and $B \rightarrow \rho \rho$ decays, one can find that $\text{BR}(B^0 \rightarrow a_1^+ a_1^-) > \text{BR}(B^+ \rightarrow a_1^+ a_1^0) > \text{BR}(B^0 \rightarrow a_1^0 a_1^0)$ in the pQCD approach. Moreover, like $B^0 \rightarrow a_1^{\pm} \pi^{\mp}$ decay [37], in principle, $B^0 \rightarrow a_1^+ a_1^-$ can be utilized to provide an independent measurement of the CKM angle α [6]. Certainly, the currently available statistics is too low to perform such an analysis on the angle of α from the current generation of B factories. But, potentially, a new generation of Super flavor factories(SuperB) are expected to achieve the result with a high luminosity $\gtrsim 10^{36} \text{cm}^{-2} \text{s}^{-1}$ [38, 39].

Now let's turn to analyze the phenomenologies of $B \rightarrow b_1 b_1$ decays. One can find that

the pQCD predictions for BRs of $B \rightarrow b_1 b_1$ decays are

$$\left. \begin{aligned} \text{BR}(B^0 \rightarrow b_1^+ b_1^-) &= 21.4_{-12.6}^{+19.1} \times 10^{-6}, \\ \text{BR}(B^+ \rightarrow b_1^+ b_1^0) &= 7.6_{-4.6}^{+7.2} \times 10^{-6}, \\ \text{BR}(B^0 \rightarrow b_1^0 b_1^0) &= 29.0_{-18.1}^{+29.1} \times 10^{-6}; \end{aligned} \right\} \quad (\text{In pQCD}) \quad (74)$$

and that in the QCDF approach,

$$\left. \begin{aligned} \text{BR}(B^0 \rightarrow b_1^+ b_1^-) &= 1.0_{-0.8}^{+15.8} \times 10^{-6}, \\ \text{BR}(B^+ \rightarrow b_1^+ b_1^0) &= 1.4_{-1.0}^{+3.8} \times 10^{-6}, \\ \text{BR}(B^0 \rightarrow b_1^0 b_1^0) &= 3.2_{-2.4}^{+12.3} \times 10^{-6}. \end{aligned} \right\} \quad (\text{In QCDF}) \quad (75)$$

in which various errors have been added in quadrature too. Though the central values of the CP-averaged BRs for $B \rightarrow b_1 b_1$ decays in the pQCD approach are much larger than those in QCD factorization, they are roughly consistent with each other within large errors and in the order of $10^{-6} \sim 10^{-5}$. It will be of great interest to measure these theoretical predictions to test pQCD and QCDF approaches experimentally.

From the theoretical predictions presented in Tables I-III, some discussions on the CP-averaged BRs for $B \rightarrow b_1 b_1$ decays are given as follows:

1. Because of charge conjugation invariance, the decay constant of the 1P_1 neutral meson b_1^0 must be zero. In the isospin limit, the decay constant of the charged b_1 vanishes due to the fact that the b_1 has even G-parity and that the relevant weak axial-vector current is odd under G transformation. Hence, $f_{b_1^\pm}$ is very small in reality. In the numerical calculations, we adopted $f_{b_1^\pm} = \mp(0.0028 \pm 0.0026)f_{b_1}$ [3].
2. In principle, because of either very small or vanishing decay constant of meson b_1 , the BRs of $B \rightarrow b_1 b_1$ decays should be significantly suppressed by comparing with the $B \rightarrow a_1 a_1$ ones as naive anticipation. However, as shown in Eqs. (13)-(22), the $b_1(^1P_1)$ meson has the rather different hadron dynamics from its 3P_1 partner, the

TABLE III. Same as Table I but for $B^0 \rightarrow a_1^0 a_1^0, b_1^0 b_1^0$ decays.

Decay Channels		$B^0 \rightarrow a_1^0 a_1^0$			$B^0 \rightarrow b_1^0 b_1^0$		
Parameter	Definition	This work	QCDF	Experiment	This work	QCDF	Experiment
BR(10^{-6})	$\Gamma/\Gamma_{\text{total}}$	$2.2_{-0.5-1.0-0.1}^{+0.6+1.6+0.1}$	$0.5_{-0.2-0.0}^{+0.8+9.3}$	—	$29.0_{-6.9-16.6-2.2}^{+7.7+27.9+3.1}$	$3.2_{-2.3-0.8}^{+5.6+11.0}$	—
f_L	$ \mathcal{A}_L ^2$	$0.12_{-0.01-0.02-0.01}^{+0.01+0.02+0.00}$	$0.60_{-0.70}^{+0.00}$	—	≈ 1.00	$0.95_{-0.80}^{+0.02}$	—
$f_{ }$	$ \mathcal{A}_{ } ^2$	$0.49_{-0.01-0.01-0.00}^{+0.00+0.00+0.00}$	—	—	≈ 0.00	—	—
f_\perp	$ \mathcal{A}_\perp ^2$	$0.40_{-0.01-0.02-0.01}^{+0.00+0.01+0.00}$	—	—	≈ 0.00	—	—
$\phi_{ }(\text{rad})$	$\pi + \arg \frac{\mathcal{A}_{ }}{\mathcal{A}_L}$	$3.58_{-0.06-0.92-0.05}^{+0.05+0.01+0.06}$	—	—	$4.20_{-0.02-0.19-0.00}^{+0.03+0.09+0.04}$	—	—
$\phi_\perp(\text{rad})$	$\pi + \arg \frac{\mathcal{A}_\perp}{\mathcal{A}_L}$	$3.64_{-0.07-0.99-0.04}^{+0.07+0.02+0.06}$	—	—	$4.24_{-0.01-0.15-0.00}^{+0.03+0.08+0.04}$	—	—
$\Delta\phi_{ }(\text{rad})$	$\frac{\phi_{ } - \phi_{ }}{2}$	$0.77_{-0.07-1.52-0.09}^{+0.10+0.02+0.07}$	—	—	$-0.32_{-0.06-0.24-0.00}^{+0.08+0.16+0.09}$	—	—
$\Delta\phi_\perp(\text{rad})$	$\frac{\phi_\perp - \phi_\perp - \pi}{2}$	$-0.83_{-0.06-1.50-0.08}^{+0.08+0.02+0.06}$	—	—	$-1.85_{-0.05-0.19-0.00}^{+0.06+0.13+0.07}$	—	—
$\mathcal{A}_{CP}^{\text{dir}}$	$\frac{\Gamma - \bar{\Gamma}}{\Gamma + \bar{\Gamma}}$	$-0.78_{-0.04-0.00-0.01}^{+0.07+0.00+0.03}$	—	—	$-0.03_{-0.01-0.00-0.01}^{+0.02+0.00+0.02}$	—	—
$\mathcal{A}_{CP}^{\text{dir}, L}$	$\frac{\bar{f}_L - f_L}{f_L + f_L}$	$0.20_{-0.55-0.05-0.01}^{+0.09+0.05+0.00}$	—	—	$-0.03_{-0.02-0.00-0.01}^{+0.02+0.00+0.02}$	—	—
$\mathcal{A}_{CP}^{\text{dir}, }$	$\frac{f_{ } - \bar{f}_{ }}{f_{ } + \bar{f}_{ }}$	$-0.91_{-0.04-0.00-0.01}^{+0.09+0.00+0.04}$	—	—	$0.19_{-0.10-0.34-0.15}^{+0.00+0.30+0.00}$	—	—
$\mathcal{A}_{CP}^{\text{dir}, \perp}$	$\frac{\bar{f}_\perp - f_\perp}{f_\perp + \bar{f}_\perp}$	$-0.90_{-0.04-0.00-0.01}^{+0.10+0.00+0.04}$	—	—	$0.23_{-0.10-0.33-0.15}^{+0.01+0.30+0.00}$	—	—

TABLE IV. The decay amplitudes(in unit of 10^{-3} GeV³) of the $B^0 \rightarrow a_1^+ a_1^-, b_1^+ b_1^-$ channels with three polarizations, where only the central values are quoted for clarification.

Channel	$B^0 \rightarrow a_1^+ a_1^-$							
Decay Amplitudes	\mathcal{A}_{fs}^T	\mathcal{A}_{fs}^P	\mathcal{A}_{nfs}^T	\mathcal{A}_{nfs}^P	\mathcal{A}_{nfa}^T	\mathcal{A}_{nfa}^P	\mathcal{A}_{fa}^T	\mathcal{A}_{fa}^P
L	$3.23 + i8.36$	$-0.82 + i0.34$	$-0.16 - i0.33$	$0.03 - i0.01$	$0.47 + i0.09$	$-0.11 + i0.29$	~ 0.00	$0.31 + i0.21$
N	$0.76 + i1.98$	$-0.19 + i0.08$	$0.28 + i0.33$	$-0.03 + i0.03$	$0.02 + i0.01$	$-0.00 + i0.01$	~ 0.00	$-0.41 - i0.61$
T	$1.46 + i3.77$	$-0.36 + i0.15$	$0.57 + i0.71$	$-0.06 + i0.05$	~ 0.00	~ 0.00	$-0.02 - i0.00$	$0.81 - i1.21$
Channel	$B^0 \rightarrow b_1^+ b_1^-$							
Decay Amplitudes	\mathcal{A}_{fs}^T	\mathcal{A}_{fs}^P	\mathcal{A}_{nfs}^T	\mathcal{A}_{nfs}^P	\mathcal{A}_{nfa}^T	\mathcal{A}_{nfa}^P	\mathcal{A}_{fa}^T	\mathcal{A}_{fa}^P
L	$-0.01 - i0.02$	~ 0.00	$-1.10 + i3.50$	$-0.36 - i0.09$	$0.52 + i1.89$	$-1.26 + i0.42$	$-0.01 - i0.00$	$-1.03 - i0.73$
N	$0.43 + i1.12$	$-0.11 + i0.05$	$0.14 - i0.12$	$0.01 + i0.02$	$-0.02 + i0.01$	~ 0.00	~ 0.00	$0.17 + i0.13$
T	$0.81 + i2.09$	$-0.21 + i0.09$	$0.32 - i0.21$	$0.02 + i0.04$	~ 0.00	~ 0.00	$0.01 - i0.00$	$0.35 + i0.29$

a_1 meson. Correspondingly, one can find the induced anomaly in the theoretical pQCD predictions on the CP-averaged BRs and other physical observables shown in Tables I-III.

3. The $B \rightarrow b_1 b_1$ decays receive dominantly large contributions arising from the non-factorizable spectator diagrams, which result in the large CP-averaged BRs. To clarify this point more clearly, we present the decay amplitudes numerically for every topology with three polarizations in the Tables IV-VI, where only the central values are quoted.
4. Moreover, the BRs of the $B \rightarrow b_1 b_1$ decays exhibit an interesting pattern highly different from that of $B \rightarrow a_1 a_1$ ones. In terms of the central values in the pQCD approach as listed in Tables I-III, one can observe that $\text{BR}(B^0 \rightarrow b_1^0 b_1^0) > \text{BR}(B^0 \rightarrow b_1^+ b_1^-) > \text{BR}(B^+ \rightarrow b_1^+ b_1^0)$, while $\text{BR}(B^0 \rightarrow a_1^0 a_1^0) < \text{BR}(B^+ \rightarrow a_1^+ a_1^0) < \text{BR}(B^0 \rightarrow a_1^+ a_1^-)$. Meanwhile, one can also find that $\text{BR}(B^0 \rightarrow b_1^0 b_1^0) > \text{BR}(B^+ \rightarrow b_1^+ b_1^0) > \text{BR}(B^0 \rightarrow b_1^+ b_1^-)$, while $\text{BR}(B^0 \rightarrow a_1^0 a_1^0) < \text{BR}(B^+ \rightarrow a_1^+ a_1^0) < \text{BR}(B^0 \rightarrow a_1^+ a_1^-)$ in the QCDF approach [3]. The confirmation of these interesting relations through the relevant experiments may shed light on the QCD dynamics involved in these considered channels.
5. Although the components of $B \rightarrow b_1 b_1$ decays at the quark level are same as that of $B \rightarrow \rho \rho$ and $B \rightarrow a_1 a_1$ decays, the different phenomenologies have been shown(See Tables I-III) because of the different QCD behavior between a_1 and b_1 mesons. One can therefore expect that $B \rightarrow b_1 b_1$ decays will imply some new information on the CKM unitary angle, reliability of pQCD approach, and so on.

As mentioned in the above, our pQCD prediction on the BR of $B^0 \rightarrow a_1^+ a_1^-$ decay is consistent with the data reported by BaBar Collaboration very recently. Though the theoretical errors are a bit large, the central value of this channel can still be employed to roughly estimate the BRs of other decay modes. Here we define four parameters, say, " R_{aa}^{0+} ", " R_{bb}^{0+} ", " R_{ab}^{00} " and " R_{ab}^{++} ", as follows,

$$R_{aa}^{0+} \equiv \frac{\tau_{B^+}}{\tau_{B^0}} \cdot \frac{\text{BR}(B^0 \rightarrow a_1^+ a_1^-)}{\text{BR}(B^+ \rightarrow a_1^+ a_1^0)} \approx 2.7, \quad R_{bb}^{0+} \equiv \frac{\tau_{B^+}}{\tau_{B^0}} \cdot \frac{\text{BR}(B^0 \rightarrow b_1^+ b_1^-)}{\text{BR}(B^+ \rightarrow b_1^+ b_1^0)} \approx 3.0; \quad (76)$$

TABLE V. The decay amplitudes(in unit of 10^{-3} GeV^3) of the $B^+ \rightarrow a_1^+ a_1^0, b_1^+ b_1^0$ channels with three polarizations, where only the central values are quoted for clarification.

Channel	$B^+ \rightarrow a_1^+ a_1^0$							
Decay Amplitudes	\mathcal{A}_{fs}^T	\mathcal{A}_{fs}^P	\mathcal{A}_{nfs}^T	\mathcal{A}_{nfs}^P	\mathcal{A}_{nfa}^T	\mathcal{A}_{nfa}^P	\mathcal{A}_{fa}^T	\mathcal{A}_{fa}^P
L	$1.98 + i5.13$	$-0.18 + i0.07$	$0.18 + i0.34$	$-0.01 + i0.00$	—	—	—	—
N	$0.48 + i1.25$	$-0.04 + i0.02$	$-0.25 - i0.27$	$0.01 - i0.01$	—	—	—	—
T	$0.92 + i2.37$	$-0.08 + i0.03$	$-0.49 - i0.60$	$0.01 - i0.01$	—	—	—	—

Channel	$B^+ \rightarrow b_1^+ b_1^0$							
Decay Amplitudes	\mathcal{A}_{fs}^T	\mathcal{A}_{fs}^P	\mathcal{A}_{nfs}^T	\mathcal{A}_{nfs}^P	\mathcal{A}_{nfa}^T	\mathcal{A}_{nfa}^P	\mathcal{A}_{fa}^T	\mathcal{A}_{fa}^P
L	$-0.01 - i0.01$	~ 0.00	$0.59 - i3.30$	$0.11 - i0.02$	—	—	—	—
N	$0.26 + i0.68$	$-0.02 + i0.01$	$-0.09 + i0.10$	~ 0.00	—	—	—	—
T	$0.49 + i1.27$	$-0.04 + i0.02$	$-0.20 + i0.20$	$-0.01 - i0.01$	—	—	—	—

$$R_{ab}^{00} \equiv \frac{\text{BR}(B^0 \rightarrow a_1^+ a_1^-)}{\text{BR}(B^0 \rightarrow b_1^+ b_1^-)} \approx 2.6, \quad R_{ab}^{++} \equiv \frac{\text{BR}(B^+ \rightarrow a_1^+ a_1^0)}{\text{BR}(B^+ \rightarrow b_1^+ b_1^0)} \approx 2.8. \quad (77)$$

We expect the above four ratios could be tested at the ongoing LHC and forthcoming Super-B experiments.

Finally, we should stress that both of the color-suppressed modes $B^0 \rightarrow a_1^0 a_1^0$ and $B^0 \rightarrow b_1^0 b_1^0$ themselves exhibit the dramatically different phenomenologies. Similar to $B^0 \rightarrow \pi^0 \pi^0, \pi^0 \rho^0, \rho^0 \rho^0$ decays³, $B^0 \rightarrow a_1^0 a_1^0$ and $b_1^0 b_1^0$ decays are closely related to the color-suppressed tree amplitudes $C^4 \propto a_2 (= C_1 + C_2/3)$, where C_1 and C_2 are Wilson coefficients. At leading order, the sign of C_2 is positive while the sign of C_1 is negative, which can cancel each other mostly. For example, the numerical result of a_2 is about 1.1×10^{-3} when the running hard scale is taken at $\mu = 2.5 \text{ GeV}$ [19]. Furthermore, one can easily find from the Table VI that the tree contributions \mathcal{A}_{fs}^T and \mathcal{A}_{nfs}^T from factorizable spectator and nonfactorizable spectator diagrams cancel each other significantly for $B^0 \rightarrow a_1^0 a_1^0$ channel. Thus $\text{BR}(B^0 \rightarrow a_1^0 a_1^0)$ is rather small relative to $\text{BR}(B^0 \rightarrow a_1^+ a_1^-)$ and $\text{BR}(B^+ \rightarrow a_1^+ a_1^0)^5$. It should be stressed that the small quantity a_2 in $B^0 \rightarrow b_1^0 b_1^0$ need not to be considered seriously because the decay constant $f_{b_1^0}$ is exact zero. But, the resulting $\text{BR}(B^0 \rightarrow b_1^0 b_1^0)$ is such large that reaching 29.0×10^{-6} numerically. It will be highly interesting to measure this rate to test the availability of pQCD approach in the channels with 1P_1 mesons.

³ As for the color-suppressed processes in the decays of B mesons, which have been extensively studied in plenties of literatures with various of methods and/or schemes within and beyond the standard model. However, to our best knowledge, they seem to be a longstanding "puzzle" in B physics because one can not resolve it self-consistently in the current approaches/methods.

⁴ Unfortunately, up to now, the color-suppressed tree amplitude C seems to be an important but the least understood quantity in B meson decays [24]

⁵ Recently, the authors in Ref. [24] proposed a solution to the $B \rightarrow \pi\pi$ puzzle by considering the contributions arising from "Glauber-gluon-region". However, it is worth mentioning that this class of contributions may make very little effects to the results on the considered $B \rightarrow a_1^0 a_1^0, b_1^0 b_1^0$ decays in the present work, which because, as argued in the literature, the Glauber effects can only contribute significantly to the pion but much less to the ρ meson.

TABLE VI. The decay amplitudes(in unit of 10^{-3} GeV^3) of the $B^0 \rightarrow a_1^0 a_1^0, b_1^0 b_1^0$ channels with three polarizations, where only the central values are quoted for clarification.

Channel	$B^0 \rightarrow a_1^0 a_1^0$							
Decay Amplitudes	\mathcal{A}_{fs}^T	\mathcal{A}_{fs}^P	\mathcal{A}_{nfs}^T	\mathcal{A}_{nfs}^P	\mathcal{A}_{nfa}^T	\mathcal{A}_{nfa}^P	\mathcal{A}_{fa}^T	\mathcal{A}_{fa}^P
L	$0.30 + i0.79$	$-0.40 + i0.17$	$-0.28 - i0.58$	$0.03 - i0.01$	$0.31 + i0.07$	$-0.08 + i0.20$	~ 0.00	$0.22 + i0.14$
N	$0.06 + i0.15$	$-0.09 + i0.04$	$0.45 + i0.51$	$-0.03 + i0.02$	$0.02 + i0.01$	~ 0.00	~ 0.00	$-0.29 - i0.43$
T	$0.12 + i0.30$	$-0.17 + i0.07$	$0.88 + i1.10$	$-0.06 + i0.05$	~ 0.00	~ 0.00	$-0.01 - i0.00$	$-0.59 - i0.86$
Channel	$B^0 \rightarrow b_1^0 b_1^0$							
Decay Amplitudes	\mathcal{A}_{fs}^T	\mathcal{A}_{fs}^P	\mathcal{A}_{nfs}^T	\mathcal{A}_{nfs}^P	\mathcal{A}_{nfa}^T	\mathcal{A}_{nfa}^P	\mathcal{A}_{fa}^T	\mathcal{A}_{fa}^P
L	0.00	0.00	$-1.34 + i5.77$	$-0.30 - i0.12$	$0.34 + i1.32$	$-0.90 + i0.31$	~ 0.00	$-0.73 - i0.52$
N	$0.04 + i0.11$	$-0.05 + i0.02$	$0.19 - i0.18$	$0.01 + i0.01$	$-0.01 + i0.01$	~ 0.00	~ 0.00	$0.12 + i0.10$
T	$0.08 + i0.21$	$-0.10 + i0.04$	$0.42 - i0.35$	$0.02 + i0.03$	~ 0.00	~ 0.00	$0.01 - i0.00$	$0.25 + i0.20$

B. Polarization Fractions

We have also computed the polarization fractions for $B \rightarrow a_1 a_1$ and $b_1 b_1$ decay modes. Based on the helicity amplitudes (24), we can define the transversity amplitudes as

$$\mathcal{A}_L = -\xi m_B^2 \mathcal{M}_L, \quad \mathcal{A}_{\parallel} = \xi \sqrt{2} m_B^2 \mathcal{M}_N, \quad \mathcal{A}_{\perp} = \xi r_2 r_3 \sqrt{2(r^2 - 1)} m_B^2 \mathcal{M}_T. \quad (78)$$

for the longitudinal, parallel, and perpendicular polarizations, respectively, with the normalization factor $\xi = \sqrt{G_F^2 \mathbf{P}_c / (16\pi m_B^2 \Gamma)}$ and the ratio $r = P_2 \cdot P_3 / (m_B^2 r_2 r_3)$. These amplitudes satisfy the relation,

$$|\mathcal{A}_L|^2 + |\mathcal{A}_{\parallel}|^2 + |\mathcal{A}_{\perp}|^2 = 1. \quad (79)$$

following the summation in Eq. (70). The polarization fractions f_L, f_{\parallel} and f_{\perp} can thus be read as,

$$f_{L(\parallel, \perp)} \equiv \frac{|\mathcal{A}_{L(\parallel, \perp)}|^2}{|\mathcal{A}_L|^2 + |\mathcal{A}_{\parallel}|^2 + |\mathcal{A}_{\perp}|^2} = |\mathcal{A}_{L(\parallel, \perp)}|^2, \quad (80)$$

The numerical results of fractions with three polarizations for $B \rightarrow a_1 a_1$ and $B \rightarrow b_1 b_1$ decays in the pQCD approach have been presented in Tables I-III. Based on these values, we give some phenomenological analysis:

1. As discussed in Sec. IV A, the prediction on $\text{BR}(B^0 \rightarrow a_1^+ a_1^-)$ with pQCD and QCDF approach, respectively, is in good agreement with the measurement given by BaBar collaboration. However, the fraction of longitudinal polarization for $B^0 \rightarrow a_1^+ a_1^-$ is not the case. Theoretically, this considered channel is dominated by the longitudinal contributions,

$$f_L(B^0 \rightarrow a_1^+ a_1^-)_{\text{pQCD}} = 0.76_{-0.04}^{+0.03}, \quad (81)$$

$$f_L(B^0 \rightarrow a_1^+ a_1^-)_{\text{QCDF}} = 0.64_{-0.17}^{+0.07}; \quad (82)$$

and f_L predicted in pQCD and QCDF are very close to each other; on the other hand, experimentally,

$$f_L(B^0 \rightarrow a_1^+ a_1^-)_{\text{Exp.}} = 0.31_{-0.24}^{+0.24}. \quad (83)$$

it seems to be governed by the transverse ones. But, it should be mentioned that the measurement performed by BaBar collaboration still have very large errors and should be greatly improved, in order to test the theoretical predictions in the near future.

2. Because the QCD behavior of axial-vector a_1 meson and that of vector ρ meson are analogous to each other, the numerical results show the similar pattern of longitudinal polarization between $B \rightarrow a_1 a_1$ and $B \rightarrow \rho\rho$ [33, 34] decays: $B^0 \rightarrow a_1^\pm a_1^\mp$ and $B^\pm \rightarrow a_1^\pm a_1^0$ decays are dominated by the longitudinal component, reaching around 76% and 91%, respectively, while $B^0 \rightarrow a_1^0 a_1^0$ is governed by the transverse one at leading order, $f_L \approx 12\%$. Maybe the situation for $B^0 \rightarrow a_1^0 a_1^0$ will be highly improved after taking the higher QCD corrections into account. (See $B^0 \rightarrow \rho^0 \rho^0$ [32] for example.)
3. Similar to $B^0 \rightarrow a_1^+ a_1^-$ and $B^+ \rightarrow a_1^+ a_1^0$ modes, $B^0 \rightarrow b_1^+ b_1^-$ and $B^+ \rightarrow b_1^+ b_1^0$ ones are also dominated by the longitudinal polarization components. However, dramatically different from $B^0 \rightarrow a_1^0 a_1^0$ decay, $B^0 \rightarrow b_1^0 b_1^0$ channel is absolutely governed by the longitudinal polarization contributions, say, $f_L \approx 100\%$.
4. For a clear clarification to the polarization fractions, we have listed the contributions from every topology with three polarizations in the Tables IV-VI. Generally speaking, from Tables IV-VI, one can find that relative to $B \rightarrow a_1 a_1$ decays, all three $B \rightarrow b_1 b_1$ decays suffer from large nonfactorizable spectator tree contributions in the longitudinal component, which therefore lead to the dominance of longitudinal polarization fraction. In contrast to $B^0 \rightarrow b_1^0 b_1^0$ decay, $B^0 \rightarrow a_1^0 a_1^0$ channel receives a bit large contributions from nonfactorizable spectator tree diagrams in both of transverse polarizations.

We expect the above observations would be tested by the future experiments, then could provide more information for understanding the underlying helicity structure in these types of decays.

C. Effects of Nonfactorizable Spectator and Annihilation Contributions

To see whether weak annihilation contributions play important role in these considered decay modes, we test the CP-averaged BRs and longitudinal polarization fraction by neglecting the annihilation diagrams, which can not be perturbatively calculated in the QCDF approach. Moreover, as claimed in the references within the framework of QCDF, the hard spectator scattering contributions also suffer from endpoint singularities at the level of twist-3. In other words, the calculations with these terms in the QCDF need always the adjustments based on the measurements at relevant experiments.

Without the annihilation contributions in both $B^0 \rightarrow a_1^+ a_1^-$ and $B^0 \rightarrow a_1^0 a_1^0$ decays, we find the following CP-averaged BRs and longitudinal polarization fractions through the numerical evaluations in the pQCD approach,

$$\text{BR}(B^0 \rightarrow a_1^+ a_1^-) \approx 51.0 \times 10^{-6}, \quad f_L(B^0 \rightarrow a_1^+ a_1^-) \approx 0.77; \quad (84)$$

$$\text{BR}(B^0 \rightarrow a_1^0 a_1^0) \approx 1.5 \times 10^{-6}, \quad f_L(B^0 \rightarrow a_1^0 a_1^0) \approx 0.07. \quad (85)$$

which means that the annihilation contributions account for a small ratio and could be neglected safely in $B^0 \rightarrow a_1^+ a_1^-$ mode, while it is not the case in the decay of $B^0 \rightarrow a_1^0 a_1^0$. When we neglect the decay amplitudes arising from both of nonfactorizable spectator diagrams and annihilation ones, the numerical results for the CP-averaged BRs and longitudinal polarization fractions of $B \rightarrow a_1 a_1$ decays are as follows:

$$\text{BR}(B^0 \rightarrow a_1^+ a_1^-) \approx 49.6 \times 10^{-6}, \quad f_L(B^0 \rightarrow a_1^+ a_1^-) \approx 0.84; \quad (86)$$

$$\text{BR}(B^+ \rightarrow a_1^+ a_1^0) \approx 20.1 \times 10^{-6}, \quad f_L(B^0 \rightarrow a_1^+ a_1^0) \approx 0.84; \quad (87)$$

$$\text{BR}(B^0 \rightarrow a_1^0 a_1^0) \approx 0.5 \times 10^{-6}, \quad f_L(B^0 \rightarrow a_1^0 a_1^0) \approx 0.88. \quad (88)$$

One can find that the nonfactorizable spectator contributions in the $B^0 \rightarrow a_1^+ a_1^-$ and $B^+ \rightarrow a_1^+ a_1^0$ modes are so small that they could be neglected, while that in $B^0 \rightarrow a_1^0 a_1^0$ is large and play an important role. This phenomenon can be easily found from the decay amplitudes shown in Tables IV-VI. In the above Eqs. (84)-(88), only the central values are quoted for clarification.

Similarly, we predict the CP-averaged BRs and longitudinal polarization fractions without the factorizable and nonfactorizable annihilation diagrams for $B^0 \rightarrow b_1^+ b_1^-, b_1^0 b_1^0$ decays,

$$\text{BR}(B^0 \rightarrow b_1^+ b_1^-) \approx 9.5 \times 10^{-6}, \quad f_L(B^0 \rightarrow b_1^+ b_1^-) \approx 0.74; \quad (89)$$

$$\text{BR}(B^0 \rightarrow b_1^0 b_1^0) \approx 18.7 \times 10^{-6}, \quad f_L(B^0 \rightarrow b_1^0 b_1^0) \approx 0.99. \quad (90)$$

which means that there should exist large contributions from annihilation diagrams in these two decays. Meanwhile, they also indicate that there are large nonfactorizable spectator diagrams [1] due to the fact of large longitudinal polarization fractions and extremely small or vanished decay constant in the longitudinal twist-2 wave function. By considering only factorizable emission diagrams in Fig. 1, the predicted BRs in the pQCD approach are determined completely by the transverse components because the longitudinal contributions from Fig. 1(a) and 1(b) are sharply suppressed by the tiny or zero decay constant,

$$\text{BR}(B^0 \rightarrow b_1^+ b_1^-) \approx 2.6 \times 10^{-6}, \quad f_L(B^0 \rightarrow b_1^+ b_1^-) \approx 0.0; \quad (91)$$

$$\text{BR}(B^+ \rightarrow b_1^+ b_1^0) \approx 1.0 \times 10^{-6}, \quad f_L(B^0 \rightarrow b_1^+ b_1^0) \approx 0.0; \quad (92)$$

$$\text{BR}(B^0 \rightarrow b_1^0 b_1^0) \approx 3.0 \times 10^{-8}, \quad f_L(B^0 \rightarrow b_1^0 b_1^0) \approx 0.0. \quad (93)$$

which exhibit evidently the dominated spectator and/or annihilation contributions involved in the $B \rightarrow b_1 b_1$ channels. Notice that for $B^0 \rightarrow b_1^0 b_1^0$ the CP-averaged branching ratio is significantly small just because the emission decay amplitudes are proportional to the combined Wilson coefficient a_2 in both transverse polarizations.

D. Direct CP-violating Asymmetries

Now we turn to the evaluations of the CP-violating asymmetries for $B \rightarrow a_1 a_1$ and $b_1 b_1$ decays in the pQCD approach. It is conventional to combine the three polarization fractions in Eq. (80) with those of its CP-conjugate \bar{B} decay, and to quote the six resulting observables corresponding to transversity amplitudes as direct induced CP asymmetries⁶ [40].

⁶ The direct CP asymmetries in transversity basis can be defined as

$$\mathcal{A}_{CP}^{\text{dir}, \alpha} = \frac{\bar{f}_\alpha - f_\alpha}{\bar{f}_\alpha + f_\alpha}, (\alpha = L, \parallel, \perp) \quad (94)$$

where the definition of \bar{f} is same as that in Eq.(80) but for the corresponding \bar{B} decay.

As for the direct CP-violating asymmetry in these considered modes, considering the involved three polarizations, whose definitions are as follows,

$$\mathcal{A}_{CP}^{\text{dir}} \equiv \frac{\bar{\Gamma} - \Gamma}{\bar{\Gamma} + \Gamma} = \frac{|\bar{M}(\bar{B} \rightarrow \bar{f}_{\text{final}})|^2 - |M(B \rightarrow f_{\text{final}})|^2}{|\bar{M}(\bar{B} \rightarrow \bar{f}_{\text{final}})|^2 + |M(B \rightarrow f_{\text{final}})|^2}, \quad (95)$$

where Γ and M denote the decay rate and decay amplitude of $B \rightarrow a_1 a_1, b_1 b_1$ decays, respectively, and $\bar{\Gamma}$ and \bar{M} are the charge conjugation one correspondingly.

Based on the above definitions on direct CP-violating asymmetry and numerical calculations in the pQCD approach (see Tables I-III), some remarks are as follows:

1. The direct CP asymmetries for $B \rightarrow a_1 a_1$ decays in the pQCD approach can be read as,

$$\mathcal{A}_{CP}^{\text{dir}}(B^0 \rightarrow a_1^\pm a_1^\mp) \approx -0.04 \pm 0.01, \quad (96)$$

$$\mathcal{A}_{CP}^{\text{dir}}(B^\pm \rightarrow a_1^\pm a_1^0) \approx 0.00, \quad (97)$$

$$\mathcal{A}_{CP}^{\text{dir}}(B^0 \rightarrow a_1^0 a_1^0) \approx -0.78_{-0.04}^{+0.08}. \quad (98)$$

which are very similar to those in the $B \rightarrow \rho\rho$ decays [34] correspondingly, where the various errors as specified have been added in quadrature.

2. As for the direct CP-violating asymmetries of $B \rightarrow b_1 b_1$ decays,

$$\mathcal{A}_{CP}^{\text{dir}}(B^0 \rightarrow b_1^\pm b_1^\mp) \approx -0.00_{-0.04}^{+0.01}, \quad (99)$$

$$\mathcal{A}_{CP}^{\text{dir}}(B^\pm \rightarrow b_1^\pm b_1^0) \approx 0.00, \quad (100)$$

$$\mathcal{A}_{CP}^{\text{dir}}(B^0 \rightarrow b_1^0 b_1^0) \approx -0.03_{-0.01}^{+0.03}. \quad (101)$$

One can find that the numerical results in the pQCD approach at leading order are very small, even to be zero within uncertainties as presented in Tables I-III.

3. Meanwhile, we calculate the direct CP-violating asymmetries in every polarization and give the results in the pQCD approach as

$$\mathcal{A}_{CP}^{\text{dir},L} = 0.11_{-0.02}^{+0.02}, \quad \mathcal{A}_{CP}^{\text{dir},||} = -0.52_{-0.10}^{+0.13}, \quad \mathcal{A}_{CP}^{\text{dir},\perp} = -0.54_{-0.09}^{+0.14}; \quad (102)$$

for $B^0 \rightarrow a_1^\pm a_1^\mp$ mode, and

$$\mathcal{A}_{CP}^{\text{dir},L} = 0.20_{-0.55}^{+0.10}, \quad \mathcal{A}_{CP}^{\text{dir},||} = -0.91_{-0.04}^{+0.10}, \quad \mathcal{A}_{CP}^{\text{dir},\perp} = -0.90_{-0.04}^{+0.11}; \quad (103)$$

for $B^0 \rightarrow a_1^0 a_1^0$ channel, and

$$\mathcal{A}_{CP}^{\text{dir},L} = -0.05_{-0.05}^{+0.04}, \quad \mathcal{A}_{CP}^{\text{dir},||} = 0.34_{-0.08}^{+0.05}, \quad \mathcal{A}_{CP}^{\text{dir},\perp} = 0.38_{-0.07}^{+0.07}; \quad (104)$$

for $B^0 \rightarrow b_1^\pm b_1^\mp$ mode, and

$$\mathcal{A}_{CP}^{\text{dir},L} = -0.03_{-0.02}^{+0.03}, \quad \mathcal{A}_{CP}^{\text{dir},||} = 0.19_{-0.38}^{+0.30}, \quad \mathcal{A}_{CP}^{\text{dir},\perp} = 0.23_{-0.38}^{+0.30}; \quad (105)$$

for $B^0 \rightarrow b_1^0 b_1^0$ channel, respectively, in which the various errors as specified have also been added in quadrature. These direct CP-violating asymmetries are expected to be confronted with the relevant measurements in the future.

4. Because of the lack of strong phase from the annihilation diagrams and the rather negligible contributions just from electroweak penguin operators in nonfactorizable spectator diagrams, the direct CP violations in the $B^\pm \rightarrow a_1^\pm a_1^0$ and $b_1^\pm b_1^0$ decays is absent for every polarization naturally, which can be seen easily in Table V.

We also define another two quantities to reflect the existence of direct CP-violating asymmetries indirectly,

$$\Delta\phi_{||} = \frac{\bar{\phi}_{||} - \phi_{||}}{2} \quad \text{and} \quad \Delta\phi_{\perp} = \frac{\bar{\phi}_{\perp} - \phi_{\perp} - \pi}{2}, \quad (106)$$

where $\bar{\phi}_{||}$ and $\bar{\phi}_{\perp}$ are the CP-conjugated ones of relative phases $\phi_{||}$ and ϕ_{\perp} , respectively. Based on the definitions of transversity amplitudes, the relative phases $\phi_{||}$ and ϕ_{\perp} are defined as,

$$\phi_{||} \equiv \arg \frac{\mathcal{A}_{||}}{\mathcal{A}_L} \quad \text{and} \quad \phi_{\perp} \equiv \arg \frac{\mathcal{A}_{\perp}}{\mathcal{A}_L}, \quad (107)$$

The theoretical predictions of relative phases for $B \rightarrow a_1 a_1$ and $b_1 b_1$ modes in the pQCD approach have been presented in Tables I-III, which will be tested by the measurements at B factories, ongoing LHC, even forthcoming Super-B experiments. Note that the definitions of $\mathcal{A}_{L,||,\perp}$ as given in Eq. (78) are consistent with those in [3], except for an additional minus sign in \mathcal{A}_L , so that our definitions of the relative strong phases $\phi_{||,\perp}$ (see Tables I-III) also differ from the ones in [3] by π , which is added to cancel the additional minus sign in the definition of \mathcal{A}_L in Eq. (78).

At last, it is worth of stressing that the theoretical predictions in the pQCD approach still have large theoretical errors (See Table I for example) mainly induced by the still large uncertainties of distribution amplitudes from the shape parameter ω_B of heavy B meson and the Gegenbauer moments $a_i^{||(\perp)}$ of light axial-vector a_1 and b_1 mesons. We need the nonperturbative QCD efforts and experimental constraints to effectively reduce the errors of these essential inputs. Any progress at this aspect will help us to improve the precision of the pQCD predictions.

V. SUMMARY

In this work, we studied the charmless hadronic $B \rightarrow a_1 a_1$ and $b_1 b_1$ decays by employing the pQCD approach based on the k_T factorization theorem. We calculated not only the factorizable emission diagrams, but also the nonfactorizable spectator and annihilation ones. Our theoretical predictions in the pQCD approach will provide an important platform for testing the SM and exploring the helicity structure of these considered decays and the hadronic dynamics of the axial-vector a_1 and b_1 mesons. They can also provide more information on measuring the unitary CKM angles and understanding the decay mechanism of color-suppressed modes.

The pQCD predictions for $B \rightarrow a_1 a_1$, $b_1 b_1$ channels are displayed in Tables (I-III). From our evaluations and phenomenological analysis, we found the following results:

- The CP-averaged branching ratio of $B^0 \rightarrow a_1^+ a_1^-$ mode in the pQCD approach is in good consistency with that given by preliminary measurement and that presented in the QCDF framework, respectively, within errors.
- The pQCD predictions for the CP-averaged branching ratios of $B \rightarrow a_1 a_1, b_1 b_1$ decays are in the range of 10^{-5} to 10^{-6} , which can be easily accessed at the B factories of BaBar and Belle, running LHC, and forthcoming Super-B experiments.
- The numerical results in the pQCD approach, specifically, on the CP-averaged branching ratios and longitudinal polarization fractions of the considered $B \rightarrow a_1 a_1, b_1 b_1$ decays are basically consistent with those given in the QCDF framework, except for $f_L(B^0 \rightarrow a_1^0 a_1^0)$.
- The theoretical predictions in the pQCD approach have large uncertainties, which mainly arise from the nonperturbative input parameters with still large errors, for example, the distribution amplitudes describing the hadron dynamics of the involved mesons. We expect these inputs will be well constrained when more data become available.
- We here simply take the short-distance contributions into account in the evaluations of $B \rightarrow a_1 a_1, b_1 b_1$ decays. Maybe the final state interactions for these considered modes play an important role, more relevant studies are therefore helpful for us to provide reliable pQCD predictions.

ACKNOWLEDGMENTS

The authors would like to thank Professor Hai-Yang Cheng for helpful discussions. X. Liu is grateful to W. Wang and Y.M. Wang for their comments. This work is supported by the National Natural Science Foundation of China under Grant No. 11205072, No. 10975074, and No. 11235005, by a project funded by the Priority Academic Program Development of Jiangsu Higher Education Institutions (PAPD), and by the Research Fund of Jiangsu Normal University under Grant No. 11XLR38.

-
- [1] M. Diehl and G. Hiller, J. High Energy Phys. **06**, 067 (2001); S. Laplace and V. Shelkov, Eur. Phys. J. C **22**, 431 (2001).
 - [2] G. Calderón, J.H. Muñoz, and C.E. Vera, Phys. Rev. D **76**, 094019 (2007).
 - [3] H.Y. Cheng and K.C. Yang, Phys. Rev. D **78**, 094001 (2008); K.C. Yang, Nucl. Phys. B (Proc. Suppl.) **186**, 399 (2009).
 - [4] H.Y. Cheng and J. Smith, Ann. Rev. Nucl. Part. Sci. **59**, 215 (2009).
 - [5] B. Aubert *et al.*, (BaBar Collaboration), Phys. Rev. D **80**, 092007 (2009).
 - [6] V. Lombardo, (BaBar Collaboration), European Physical Society Europhysics Conference on High Energy Physics, July 16-22, 2009, Krakow, Poland, **PoS EPS-HEP2009**, 162 (2009).
 - [7] P. Gandini, (BaBar Collaboration), Proceedings of the DPF-2009 Conference, Detroit, MI, July 27-31, 2009, arXiv:0910.2945[hep-ex].
 - [8] K.C. Yang, J. High Energy Phys. **10**, 108 (2005); Nucl. Phys. B **776**, 187 (2007).

- [9] H.Y. Cheng and K.C. Yang, Phys. Rev. D **76**, 114020 (2007).
- [10] D. Asner *et al.*, (Heavy Flavor Averaging Group), arXiv:1010.1589[hep-ex]; and online update at <http://www.slac.stanford.edu/xorg/hfag>.
- [11] J. Schwinger, Phys. Rev. Lett. **12**, 630 (1964); M. Wirbel, B. Stech, and M. Bauer, Z. Phys. C **29**, 637 (1985); M. Bauer, B. Stech, and M. Wirbel, *ibid.* **34**, 103 (1987); L.L. Chau, H.Y. Cheng, W.K. Sze, H. Yao, and B. Tseng, Phys. Rev. D **43**, 2176 (1991); **58**, 019902(E) (1998).
- [12] M. Beneke, G. Buchalla, M. Neubert, and C.T. Sachrajda, Phys. Rev. Lett. **83**, 1914 (1999); Nucl. Phys. B **591**, 313 (2000); D.S. Du, H.J. Gong, J.F. Sun, D.S. Yang, and G.H. Zhu, Phys. Rev. D **65**, 094025 (2002).
- [13] G. Buchalla, A.J. Buras, and M.E. Lautenbacher, Rev. Mod. Phys. **68**, 1125 (1996).
- [14] Y.Y. Keum, H.N. Li, and A.I. Sanda, Phys. Lett. B **504**, 6 (2001); Phys. Rev. D **63**, 054008 (2001); C.D. Lü, K. Ukai, and M.Z. Yang, Phys. Rev. D **63**, 074009 (2001).
- [15] H.N. Li, Prog. Part. & Nucl. Phys. **51**, 85 (2003) and reference therein.
- [16] F. Ruffini, (CDF Collaboration), talk given at the Flavor Physics and CP violation 2011, May 23-27, Israel; arXiv:1107.5760[hep-ex]; M.J. Morello *et al.*, (CDF Collaboration), CDF public note 10498 (2011); T. Aaltonen *et al.*, (CDF Collaboration), arXiv:1111.0485[hep-ex].
- [17] A. Powell, (LHCb Collaboration), talk given at PANIC 2011, MIT, July 2011; V. Vagnoni, (LHCb Collaboration), LHCb-CONF-2011-042, Sept. 20, 2011.
- [18] Y. Li, C.D. Lü, Z.J. Xiao, and X.Q. Yu, Phys. Rev. D **70**, 034009 (2004).
- [19] A. Ali, G. Kramer, Y. Li, C.D. Lü, Y.L. Shen, W. Wang, and Y.M. Wang, Phys. Rev. D **76**, 074018 (2007).
- [20] Z.J. Xiao, W.F. Wang, and Y.Y. Fan, Phys. Rev. D **85**, 094003 (2012).
- [21] C.W. Chiang, M. Gronau, J.L. Rosner, and D.A. Suprun, Phys. Rev. D **70**, 034020 (2004).
- [22] Y.Y. Charng and H.N. Li, Phys. Rev. D **71**, 014036 (2005).
- [23] R. Fleischer, S. Recksiegel, and F. Schwab, Eur. Phys. J. C **51**, 55 (2007).
- [24] H.N. Li and S. Mishima, Phys. Rev. D **83**, 034023 (2011).
- [25] C.W. Bauer, S. Fleming, and M.E. Luke, Phys. Rev. D **63**, 014006 (2001); C.W. Bauer, S. Fleming, D. Pirjol, and I.W. Stewart, Phys. Rev. D **63**, 114020 (2001); C.W. Bauer and I.W. Stewart, Phys. Lett. B **516**, 134 (2001); C.W. Bauer, D. Pirjol, and I.W. Stewart, Phys. Rev. D **65**, 054022 (2002); C.W. Bauer, S. Fleming, D. Pirjol, I.Z. Rothstein, and I.W. Stewart, Phys. Rev. D **66**, 014017 (2002).
- [26] H.N. Li, Phys. Rev. D **66**, 094010 (2002).
- [27] H.N. Li and B. Tseng, Phys. Rev. D **57**, 443 (1998).
- [28] C.D. Lü and M.Z. Yang, Eur. Phys. J. C **28**, 515 (2003).
- [29] R.H. Li, C.D. Lü, and W. Wang, Phys. Rev. D **79**, 034014 (2009).
- [30] H.N. Li and H.L. Yu, Phys. Rev. Lett. **74**, 4388 (1995); Phys. Lett. B **353**, 301 (1995); Phys. Rev. D **53**, 2480 (1996).
- [31] T. Huang and X.G. Wu, Phys. Rev. D **71**, 034018 (2005).
- [32] Y. Li and C.D. Lü, Phys. Rev. D **73**, 014024 (2006).
- [33] C.H. Chen, arXiv:0601019[hep-ph].
- [34] H.N. Li and S. Mishima, Phys. Rev. D **73**, 114014 (2006).
- [35] X. Liu, Z.J. Xiao, and Z.T. Zou, arXiv:1105.5761[hep-ph] and references therein.
- [36] C. Amsler *et al.*, (Particle Data Group), Phys. Lett. B **667**, 1 (2008).

- [37] W. Wang, R.H. Li, and C.D. Lü, Phys. Rev. D **78**, 074009 (2008).
- [38] T. Gershon and A. Soni, J. Phys. G **34**, 479 (2007).
- [39] M. Bona *et al.*, (SuperB Collaboration), INFN/AE-07/2, SLAC-R-856, LAL 07-15, arXiv:0709.0451[hep-ex]; A.G. Akeroyd et al., Belle-II Collab., *Physics at Super B Factory*, arXiv:1002.5012 [hep-ex].
- [40] M. Beneke, J. Rohrer, and D.S. Yang, Nucl. Phys. B **774**, 64 (2007).